

**Best Available
Copy
for all Pictures**

AD-772 506

STUDY OF HIGH POWERED PLASMA FOR IN SITU HARD ROCK
DISINTEGRATION

HUMPHREYS CORPORATION

PREPARED FOR

ADVANCED RESEARCH PROJECTS AGENCY

21 JULY 1973

DISTRIBUTED BY:

NTIS

National Technical Information Service
U. S. DEPARTMENT OF COMMERCE

Unclassified

AD-772506

DOCUMENT CONTROL DATA - R & D		
<small>(Security classification of title, body of abstract and indexing information must be entered when the original report is classified)</small>		
1. ORIGINATING ACTIVITY (Corporate author)		2. REPORT SECURITY CLASSIFICATION
TAFE Division Humphreys Corporation Bow Road, Bow, New Hampshire 03301		Unclassified
3. REPORT TITLE		7b. GROUP
Study of High Powered Plasma for In Situ Hard Rock Disintegration Semiannual Technical Report		
4. DT Final Technical Report (1 April 1972 - 21 July 1973)		
5. AUTHOR(S) (First name, middle initial, last name)		
John W. Poole, Merle L. Thorpe		
6. REPORT DATE	7a. TOTAL NO. OF PAGES	7b. NO. OF REFS
July 21, 1973	46 83	24
8a. CONTRACT OR GRANT NO.	9a. ORIGINATOR'S REPORT NUMBER(S)	
H0220051	TAFE 7311-9	
b. PROJECT NO.	9b. OTHER REPORT NO(S) (Any other numbers that may be assigned this report)	
ARPA Order No. 1579, Amend. 3		
c. Program Code: 62710D		
10. DISTRIBUTION STATEMENT		
Distribution of this document is unlimited		
11. SUPPLEMENTARY NOTES		12. SPONSORING MILITARY ACTIVITY
		Advanced Research Projects Agency Washington, D.C. 20301
13. ABSTRACT		
<p>This contract investigated hard rock cutting using a transferred arc plasma for melting narrow, deep cuts in hard rock at high speed and removing the intervening rock by thermal fracturing. The one year experimental program resulted in the development of a cutting system capable of operating horizontally and vertically at 250-500 kW, producing continuous cuts in granite and basalt at 2-1/2 to 12 inches per minute depending on cut depth which ranged from one to nineteen inches. Thermal melting efficiencies were in the range of 20-30 percent. Results indicate significant rock fracturing will occur during the kerf cutting process due to heat buildup in the rock. Higher cutting speeds and deeper cuts appear to be possible with higher powers and are power densities. Extrapolation of the cutting data to 9,000 kW indicates tunneling speeds of 200+ feet per day could be expected with an eight foot tunnel, using 6 to 8 torches operating simultaneously.</p>		
<p>Reproduced by NATIONAL TECHNICAL INFORMATION SERVICE U.S. Department of Commerce Springfield, VA 22151</p>		

DD FORM 1473

Unclassified

Security Classification

UNCLASSIFIED

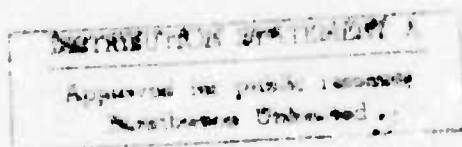
Security Classification

KEY WORDS	LINK A		LINK B		LINK C	
	MOLE	WT	MOLE	WT	MOLE	WT
Plasma rock cutting						
Tunneling						
Excavation						
High temperature rock cutting						
D.C. plasma						
Transferred arc						

UNCLASSIFIED
Security Classification

STUDY OF HIGH POWERED PLASMAS
FOR IN SITU HARD ROCK DISINTEGRATION

DDC
RECEIVED
JAN 17 1974
B



Distribution of this document is unlimited

TAFD 7311-9
July 21, 1973

FINAL TECHNICAL REPORT
1 April 1972 21 July 1973

STUDY OF HIGH POWERED PLASMAS FOR IN SITU
HARD ROCK DISINTEGRATION

Contract No. H0220051

ARPA Order No. 1579, Amendment 3
Program Code 2F10

Effective Date of Contract: 21 March 1972
Contract Expiration Date: 21 July 1973
Amount of Contract: \$59,083 (CPFF)

Principal Investigator: John Poole
(603) 224-9581

Project Director: M. L. Thorpe
(603) 224-9581

TAFD DIVISION
Humphreys Corporation
Dow Road
Bow, New Hampshire 03301

The views and conclusions contained in this document are those of the authors and should not be interpreted as necessarily representing the official policies, either expressed or implied, of the Advanced Research Projects Agency of the U.S. Government.

FORWARD

The Final Technical Report, covering the period 1 April - 31 July, 1973, was prepared by TAFA Division, Humphreys Corporation.

The work reported in this document is supported by the Advanced Research Projects Agency of the Department of Defense, and is monitored by the Bureau of Mines under Contract No. H0220051.

TABLE OF CONTENTS

	<u>Page</u>
TECHNICAL REPORT SUMMARY.....	1
INTRODUCTION.....	2
GENERAL DISCUSSION.....	3
Transferred Arc Plasma Cutting.....	3
Dielectric Heating for Rock Fragmentation.....	9
EQUIPMENT USED.....	10
TEST PROCEDURE.....	11
TEST RESULTS.....	12
PROJECTED TUNNELING PERFORMANCE.....	20
CONCLUSIONS.....	22
PATENTS AND INVENTIONS.....	22
APPENDIX A: THEORETICAL CONSIDERATIONS, COMMENTS ON OTHER HEAT SOURCES AND ENERGETICS AND SPEED OF CUTTING.....	23
APPENDIX B: BACKGROUND, INTERNAL HEATING TO CREATE THERMAL INCLUSIONS VIA DIELECTRIC MEANS.....	36
APPENDIX C: SUMMARY OF DIELECTRIC HEATING INVESTIGATIONS.....	40
BIBLIOGRAPHY.....	45
TABLES AND FIGURES	

TECHNICAL REPORT SUMMARY

This program involved approximately one man year of engineering and resulted in the development of a cutting system capable of operating horizontally and vertically at 250-500 kW, producing continuous cuts in granite and basalt at 2-1/2 to 12 inches per minute depending on cut depth which ranged from one to nineteen inches. Thermal melting efficiencies were in the range of 20-30 percent. The preliminary results indicated that significant rock fracturing would occur during the kerf cutting process due to heat buildup in the rock. The data generated appears to indicate that higher cutting speeds and deeper cuts could be achieved with higher powers and arc power densities. Extrapolation of the cutting data to 9,000 kW indicates tunneling speeds of 200+ feet per day could be expected with an eight foot tunnel, probably using 6 to 8 torches operating simultaneously.

The program was primarily experimental in nature. Previous company experience and background in this field permitted use of existing cutting torches to operate at the powers indicated with minor modifications. Large blocks of granite were set up in an outdoor laboratory area where cutting tests could be simply performed. Most samples tested were eighteen inches square by four feet long with typical screening cuts lasting 1-3 minutes. Once initial parameters were established, larger samples and five-minute cutting tests were typical. Electrical heat balance measurements were simple, since d.c. power was used and heat losses to water-cooled portions of the system were less than 7%.

The system cutting performance was correlated with a simple heat transfer model which showed that cutting speed was directly related to the heat transfer from the arc saw at the leading edge of the cut and the thickness of the molten film on the surface. An unexpectedly thin film was measured with the two rocks of major interest - granite and basalt. In the case of granite, the molten film coalesced into small webs covering approximately 20% of the surface, the remainder is bare or covered by an infinitesimally thin transparent film of liquid considerably less than .001" thick. In the case of basalt, no molten film could be observed visually. Since the theoretical cutting speed is reduced drastically with small increases in film thickness, this was a fortuitous physical phenomenon.

Towards the end of the program most relevant cuts involved movement of the cutting device upwards on a vertical face to produce an 8-10" deep kerf at a traverse speed of 25"/minute on Concord gray granite. Such a system could be operated continuously in its present form and relates to the final projected system which would produce a 24" deep cut traveling at 9.6"/minute at a power of 1,500 kW per torch. It should thus be noted that a scale up of only five was required in the torch size with a speed increase of approximately three times over than run in this program. Parenthetically it should be noted that the state of the art on plasma torches is such that powers far in excess of the 1,500 kW contemplated have been operated on other applications. Cutting speeds higher than 9.6"/minute have been measured when cutting thin granite blocks. It thus appears to the investigators the higher speeds and deeper depths can be achieved with higher powers, increase of power density in the arc and addition of plasma gases which would improve heat transfer characteristics.

It would appear to the investigators that this tunneling technique warrants further investigation since preliminary estimates indicate the tunneling and excavation objectives of the National Academy of Science (9) can be reached. Furthermore, the system provides a simple non-blasting technique for not only advancing tunnels but severing concrete structures with metal reinforcing rods. These continuing tests would involve larger scale cutting and in situ tunneling environment. The major drawback appears to be the requirement of a relatively large amount of power when compared with that available in the field, however, standard power supplies are available in the construction industry capable of reaching the levels of power utilized in these tests.

INTRODUCTION

The National Academy of Sciences indicated the desirability and benefits of achieving dramatic improvements in hard rock tunneling in their report entitled, "National Research Council Committee on Rapid Excavation - Significance - Needs - Opportunities," Washington, D.C., 1968. The plasma tunneling process described here is one of the novel techniques being funded by the government to obtain a breakthrough in hard rock tunneling speed and economics.

TAFI feels a combination of a transferred arc d.c. plasma for in situ rock cutting with associated thermal fragmentation, which removes concurrently the blocks formed by the arc cutting, is an attractive hard rock tunneling concept. Figure 1 (A) depicts how a cut of suitable shape would be scribed in the tunnel face using a narrow kerf plasma melting technique. In addition, it was proposed prior to the program that two or more plasma contacts be inserted in the kerf to cause high frequency current to flow through the rock between the plasma contacts to produce auxiliary fragmentation and removal of the core - Figure 1 (B). Cutting and fragmentation would continue to be used alternatively to produce the desired tunneling.

GENERAL DISCUSSION

Transferred Arc Plasma Cutting

The major goal of this contact is the investigation of in situ transferred arc d.c. plasma cutting for melting narrow, deep cuts in hard rock at high speed. This is a standard process for high speed cutting of ferrous metals, stainless and super alloys up to about five inches thick (1, 3, 4). In the cutting of metals, the process provides heat equal to the energy gained by the electrons when they are accelerated by the anode drop, plus the convection from the hot gas stream accompanying the arc, and the radiation from the arc column and hot gas. In the work reported here, there is limited current flow through the molten material on the surface of the rock so that the dominant heating modes are radiation and convection from the plasma stream.

For most rocks, transferred arc cutting depends almost completely on melting of the rock for its successful operation. Thus, the temperature of the rock must be increased to the melting point and then enough heat must be added to allow it to flow out of the cut region under the forces present. Since a layer of molten rock separates the plasma from the rock to be heated, the importance of the properties of the molten rock becomes immediately apparent. If the molten material becomes quite fluid just above its melting temperature the molten layer will be thin and the heat conduction to the base rock will be efficient. On the

other hand, for quartzite the melting temperature is extremely high and the viscosity so high that any molten layer that forms is difficult to wash away. As a result of this and the low thermal conductivity of silica, the efficiency of heat transfer to the base rock is reduced. Thus, the viscosity of the molten material in front of the arc is a key factor in controlling the speed of transferred arc rock cutting. Rocks like quartzite may be cut most efficiently by progressive spalling rather than melting unless chemical fluxes are added to the plasma to make the molten material more fluid.

A theoretical cutting model is outlined in Appendix A. This theory predicts cutting rates as a function of the power density projected on the rock, melt thickness, and physical properties of the rock.

Cutting torch electrodes can be designed to maximize the shearing action of the gas flow and, thus, wash the molten material out of the cut. The maximum jet momentum is established at the exit of the nozzle. An analysis using the steady flow energy equation helps to put the important factors into perspective. The equation may be written in simplified form with condition one at the entrance to the nozzle duct at the cathode tip and condition two at the nozzle exit. Since the enthalpy and velocity of the gas at one can be neglected, the expression simplifies to:

$$\frac{d_1 Q_2}{dt} = \frac{dm}{dt} \left(\frac{\bar{v}_2^2}{2gJ} + h_2 \right)$$

The expression on the left is the rate of energy addition in the nozzle and is equal to the arc current times the voltage gradient times the nozzle length (assuming negligible cooling losses). The expression on the right is the mass flow rate times the kinetic energy and enthalpy at state two. Since the nozzle now being used has a choked flow throat at the exit, the velocity at two is approximately sonic velocity at the temperature of the exhaust gas stream. The voltage gradient is a weak function of pressure. Cobine (2) gives the voltage gradient proportional to pressure to the Mth power where M equals 0.31 for nitrogen and 0.16 for argon.

From this equation it is readily seen that the heat addition in the nozzle results in a contribution to the kinetic energy term and to the enthalpy of the gas. Since sonic velocity increases with temperature, an increase in the arc current produces an increase in the jet velocity and the enthalpy term. With the mass flow rate assumed constant, the momentum of the jet is increased and the viscosity of the jet is increased by the higher temperature. If, on the other hand, the arc current is maintained constant and the gas flow rate through a particular nozzle is increased, both the velocity term and the enthalpy term will drop. Evaluation of the net effect on the molten material for this case, taking into consideration the jet temperature and jet viscosity, is difficult. It is apparent that the heat addition within the nozzle should be maximized however because of the beneficial effects on velocity, temperature and jet viscosity.

At least eleven variables are associated with this plasma cutting process, with a number necessarily inter-related. In the following paragraphs each of these variables is described with an indication of its effect on the cutting process (Figure 2).

1. Arc Power - This is the product of arc voltage and current. The voltage gradient in the cut region is typically 30 to 35 volts/in. Within the arc nozzle the voltage gradient is higher (typically 125 volts/in.) because of the pressure, arc constriction and absence of seeding from the vaporized rock. Since the arc voltage is fixed for any given arc length and gas type, the real variable is current, which is adjusted by control of the d.c. power supplies.

The current level used for testing work early in this program was 550 amps, with an associated power of 225 to 250 kW. Later in the program the current was increased to the 625 amp limit of the power supplies. Power levels were typically 350 to 400 kW.

2. Length of the Torch Nozzle - As described previously, a longer nozzle heats the gas more before it exits from the torch with a consequent increase in velocity and momentum. This desirable trend must be balanced against a rise in voltage gradient within the nozzle which increases the tendency toward double arcing. Double arcing is the establishment of a current path in parallel with the main arc column, running from the cathode to the nozzle wall,

through the nozzle, and off the front face of the nozzle back to the main arc column. Because of this tendency, a compromise nozzle length must be accepted.

3. Nozzle Contour - The nozzle contour plays an important part in determining the gas heating within the nozzle since the central arc core is surrounded by a sheath of cooler gas. A number of nozzle designs were tried on this program to determine the optimum configuration for cutting rock. Generally, a straight cylindrical bore is the most versatile in allowing variations in gas flow and arc current, but for cutting rock this geometry did not produce adequate velocity. A converging-diverging configuration and a simple converging nozzle were tried. These tests revealed that the converging nozzle with the smallest cross section at the exit from the torch produced the best cutting action.

4. Exit Orifice - In addition to the internal shape of the nozzle, the diameter of the exit orifice is important since for any given gas flow rate and arc current the operating pressure within the torch is dependent on its area. The standard nozzle used on this program has an orifice 3/16 inch in diameter. During typical operation this provides a torch pressure of approximately 16 psig at the 250 kW level using 250 SCFH of gas.

5. Gas Flow Pattern - A standard technique for metal cutting involves tangentially inward injection of plasma forming gas through critical flow orifices within the torch. This produces the strongest possible vortex within the nozzle and minimizes the tendency toward double arcing. However, since the vortex extends outside the torch, the flow tends to expand more than with straight axial flow. The gas injection scheme used early in this program was a compromise between axial and tangential flow which provides a tight arc column with relative freedom from double arcing. At the higher current operating points used late in the program, it was necessary to go to the vortex injection for maximum protection against double arcing.

6. Gas Mixture - Argon is the easiest gas to work with due to its low voltage gradient and diffuse arc; however, it is quite expensive. A standard mixture for plasma metal cutting consists of argon and hydrogen. This would probably be effective for rock cutting but would be expensive as well as explosive in a mine atmosphere.

Nitrogen is another candidate and has the characteristic of a significantly higher arc voltage gradient, which should be helpful in achieving higher powers at a later date. All the cutting tests during the second half of this program utilized straight nitrogen as the torch gas.

7. Gas Flow Rate - The gas flow rate through a nozzle directly affects the pressure within the torch. The cutting process does not seem to be extremely sensitive to variations in the flow rate. Tests made at high flows through the nozzle resulted in slower cutting speeds as postulated earlier. The flow rate of nitrogen used was approximately 250 SCFH. However, it appears that a combination of higher flows with higher powers would be helpful in producing deeper more rapid cutting.

8. Stand-off - It has been found desirable to maintain the stand-off distance between the torch and the rock face at $3/4$ to 2 inches. At stand-off distances of $1/2$ inch and less there are occasional spalls of the top surface of the rock that bridge the gap between the rock and torch face, leading to double arcing.

A sheath flow around the arc has been found desirable. The relatively high momentum of the sheath gas tends to clear the leading edge of the cut so that greater stand-offs can be tolerated. The increased mixing that takes place with larger stand-offs tends to decrease the depth of penetration, however.

9. Cutting Speed - The cutting speed, along with penetration depth, are the best measures of success in hard rock tunneling. Typically, at slow speeds (300 kW) the arc cuts all the way through a six inch rock slab, producing a near vertical advancement face. As the speed is increased the bottom of the cut curves backward, with reduced vertical penetration immediately below the torch. Further increases in speed finally result in a horizontally deflected arc column which becomes so long that it exceeds the operating voltage available from the power supply (causing extinguishment). As a rule of thumb, when operating in the range of 300 kW it has been noted that successful cutting results when the lag at a depth of eight inches does not exceed two inches.

During most work on the program the torch was cutting vertically downward so that some of the hot gases within the cut region tended to flow upward around the arc column. This can result in an ionized gas bridge to the

front of the torch (double arcing). In order to avoid this tendency with the early torch configuration, a sheath of gas was introduced across the face of the torch to blow the ionized gas away. A torch with a sheath gas flow coaxially around the nozzle and an electrically isolated front end eliminated all tendency to double arc.

10. Transferred Arc Electrode - The original concept for the transferred arc anode proposed for this program is shown in Figure 3. It has been determined that a simplified anode can be utilized. A graphite rod is inserted near or into the cut in place of the right-hand arc column. The cutting arrangement used for the first part of the program is shown in Figure 4 (B), and the tunneling configuration used later in the program is shown in Figure 4 (C).

The placement of the transferred arc anode is another variable. The anode should be positioned so as to force the arc as close to the cutting face as possible. Figure 4 (C) shows the proposed tunneling configuration with the arc stretched to the anode inside the cut groove. This geometry was used very successfully during the later part of the program.

11. Fluxing - Fluxing additives can be blown into the cut region to aid in fluidizing the molten rock. An addition of 25 percent sodium to fused silica reduces the melting temperature by approximately 1000°C (6). Actual cutting tests with sodium bicarbonate demonstrated the possibility of increasing cutting speed by 25%. However, extraneous double arcing prevented sustained operation with the torch configuration used. Further work must also be directed to injecting fluxing agent into the molten rock since much of it lands on the surface and is washed away.

In reviewing this list of variables it should be readily apparent that a great deal of time could be spent investigating their interrelationships and determining the optimum cutting situation. Within the scope of this program, however, only a limited amount of optimization was possible before "freezing" the design to be combined with dielectric heating for simulated tunneling. The fact that project personnel involved had many years of experience with such arc devices accelerated the optimization studies considerably.

During the last few months on this program both an electrically floating, extra long orifice and a simple converging anode with sheath flow were available for testing. The cutting speed and depth of penetration were slightly better with the extended anode due to higher power dissipation within the nozzle. The higher voltage drop restricted its use to about a 12 inch cutting depth, so the sheath flow torch was used exclusively. For a follow-on program, an electrode set should be designed to combine the desirable features of these two, i.e. an electrically isolated front end with sheath flow, and an extended, electrically segmented nozzle, to provide even greater gas heating.

Dielectric Heating for Rock Fragmentation

Thirumalai has investigated the potential of dielectric heating of a localized inner volume of rock for thermal stress rock fragmentation (5, 7). His excellent theoretical discussion of the process plus his experimental investigations leave little question as to the potential value of the process if imbedded electrodes are used. The heated volume required for fragmentation is only a few percent of the test block volume and the electrical energy consumption is of the order of 3.5 to 6.5 kWh/m³ (5). It should be noted, however, that the thermal inclusion generated during Thirumalai's experiments were deep within the rocks using electrodes inserted in drilled holes. Thus, the compressive stresses generated in the heated region had a maximum tendency to generate tensile stresses at the surface, with resultant fracturing. Our results show when the heating takes place at the surface, and especially where there is localized surface melting, the stresses disappear in the softened material and it is more difficult to generate fracturing stresses.

The second phase of the current program was designed to investigate the use of plasma columns as contacts for dielectric heating of the blocks produced by plasma cutting. The fact that a plasma column can stretch a foot or more into a cut in the rock means that the dielectric energy can be coupled into the rock deep within the groove. This is the ideal location to achieve the maximum effect from the thermal inclusion to break away material.

The laminar flow column of argon plasma used for these experiments [Figure 5 (A and B)] has an electrical resistance of approximately one ohm. At the rock end of the column, the plasma spreads out into a zone roughly 2 inches in diameter. This zone is in intimate contact with the rock, and, in fact, some localized melting takes place at the contact point. It was hypothesized that the uniform voltage gradients that should be established at this contact point should allow the electrode to be operated at higher r.f. voltages and, consequently, at higher heating rates (details described in Appendix B). Solid metal electrodes tend to generate very high voltage gradients in the region of rough spots in the surface, and this causes severe surface arcing during dielectric heating runs.

EQUIPMENT USED

The basic device for transferred arc plasma cutting on this program was a general purpose 1,000 ampere d.c. plasma torch. The unit used was one that was available and could be readily adapted for the high power cutting operation. A special water cooled nozzle holder was designed for the front end of the torch to protect it against the cutting environment. The configuration for the tungsten cathode and the copper anode insert were subject to modification during the program, as discussed in the next section of this report. A schematic of the vertical plasma cutting setup is shown in Figure 6. Figure 7 is a photograph of the torch with a cut on Concord gray granite.

The anode used in the transferred arc circuit during this program has been a graphite rod two inches in diameter. During early cutting tests two graphite rods were used beneath the rock sample with hot gas and molten effluent streaming between them. Later, a single graphite rod was substituted and has been located in several different places relative to the cut. It is envisioned that the anode for tunneling operations will be a narrow slab of graphite which will be located near the kerf exit or protrude into the cut, as shown in Figure 4 (C) and 8. It is estimated from experience that the loss of material from the graphite anode would be about 0.01-0.03 lb/kWh during the cutting operation.

The power for the cutting operation is provided by 100 kW d.c. rectifiers. Each unit has an open circuit voltage of 320 and a rated output of 160 volts at 620 amperes. The d.c. waveform is smoothed by two large chokes in the power supply output, as shown in Figure 6. A standard spark gap high frequency generator provides the voltage for breaking down the electrode gap in the plasma generator at startup. A water cooled ballast resistor is used to limit the starting current and a knife switch opens the torch nozzle circuit once arc transfer to the graphite anode is complete. Three rectifiers were used during the first nine months on the program and four for the rest of the year.

The remainder of the transferred arc cutting setup consists of a control console (which includes switching, power control, and gas flowmeters), cutting table and torch motion device. The cutting table (Figure 7) provides the necessary support for heavy rock samples and the motion device (a Welding Apparatus Company variable speed unit, Model Mark 111). The movement was selected for controlled vertical motion which was required for the simulated tunneling operation.

Figure 9 shows a schematic of the equipment used for dielectric heating with a plasma contact. The r.f. generator for the dielectric heating is a 190 kW plate power Lepel unit with components for operation at 3-8 MHz and 12-20 MHz. Most of the work with the r.f. unit was at 5-8 MHz because of the stability of that setup. At the end of the program the high frequency grid circuit was connected and operated at 12 to 15 MHz.

TEST PROCEDURE

For transferred arc cutting, the equipment is arranged as shown in Figure 7. Cutting is initiated by the following steps. The torch is started on nitrogen in the non-transferred mode operating through the ballast resistor. Power is then turned up until the arc transfers to the steel starting wire which stretches from below the nozzle to the graphite anode. At this point the knife switch is opened in the torch nozzle circuit, the power is turned up to over 400 amps, and the nitrogen flow through the nozzle is

increased. The starter wire is melted down to stretch the arc column from the torch to the graphite (approximately an inch in front of the rock). Next, the torch motion is started at a preset speed and the cutting action commences. Since the arc is broader at the bottom, some spalling takes place in front of the graphite electrode before the material at the top of the rock is affected by the arc. Figure 10 shows the cutting operation after the arc has progressed about two inches into a 9-1/2 inch thick piece of granite.

The cuts are timed from the instant material removal starts at the top of the rock. Preset cutting speeds are maintained and the cut contour is used as one of the criteria for cut comparison. After a cut is terminated, usually after a predetermined time span, a group of measurements is made to record the cut profile. These figures, plus the notation of electrode configuration, arc current and voltage, and gas flows, constitute a complete test record. Anything unusual associated with the cut is also noted and photographs may be taken. Early in the program complete heat balances were made on the system; however, since torch losses were only 3 to 7 percent of the d.c. power supplied, these were discontinued.

TEST RESULTS

The primary activity during the first few months of the program involved the testing of various electrode geometries and gas flows in an effort to find the best combination for rock cutting. The criterion for success was the maximum cutting speed obtainable with good penetration. All cuts made during the electrode testing phase were in Concord gray granite from The John Swenson quarry. After the configuration was optimized, comparative cuts were made on the Dresser basalt, St. Cloud gray granodiorite, and Sioux quartzite, all supplied by the Bureau of Mines. During the middle portion of the investigation, work was broadened to include cutting through a discontinuity in the rock face and addition of a fluxing agent to the plasma stream. These tests are described in the following paragraphs and the comparative cuts are summarized in Table 1. Late in the program the emphasis was on higher power cutting, determining maximum cut depth obtainable with available power, and operating in the angled electrode mode [Figure 4 (C)] on a vertical rock face which was proposed for actual tunneling operations.

The plasma torch electrode investigations started with a 5/16 inch diameter nozzle insert appropriate for generating a laminar transferred flame. This configuration operates very reliably and can be used to produce an extremely hot plasma flow, but it did a disappointingly slow job of cutting. In an effort to increase the gas velocity exiting from the nozzle, and thus, the cutting speed, a converging-diverging design was tried early in the program with the throat up near the tip of the cathode. This configuration provided only a slight improvement in cutting action. The second configuration utilized a duct converging toward the exit. This provided a substantial improvement in cutting performance but caused rapid erosion of the thoriated tungsten cathode due to the increased pressure within the torch. At this point a special tungsten cathode material doped with barium, calcium and alumina was ordered. This material was selected due to its outstanding performance during a cathode research program conducted a few years ago (8). This material was found to hold up well in the 15-20 psig environment within the torch. The nozzle geometry finally selected was as long as possible and with as small an orifice as possible without producing excessive double arcing (0.75 inches long and 0.187 inch orifice). The combination provided the tightest arc column and the best cutting performance.

Of the 150-odd cuts (includes optimization tests not included in data and tables herein) that were made on the program, all but 30 used Concord gray granite. Figure 11 shows a photograph of a typical cut in this material. The cuts were intentionally terminated before the sample was severed since cut completion led to a break-up of the test sample and complicated interpretation of results.

Figure 12 shows a rendition of one side of a typical cut on granite six inches thick. The curvature at the leading edge of the cut (A) is caused by the accumulation of molten material toward the bottom of the cut and by diffusion of and loss of velocity of the cutting stream (both reduce heat transfer to the rock). This curvature can be almost eliminated by cutting slowly, and it increases with cutting speed. Since the goal was to make cuts 12 to 16 inches deep in a tunneling operation (at 300 kW), the cutting speed has been restricted to a rate that would produce this cut contour. The area indicated by arrow (B) involves a substantial kerf widening when cutting granite. This is caused, after the arc has passed, by spalling during the washing of hot gas over that

region. The spalling that has taken place to create the fracture planes at arrows (C) and (D) is typical of all of the cuts on granite. The lower edge at the entrance normally recedes more than the upper edge due to the hot gas washing back more in this area as it flows around the graphite anode. Normally, there is some fracturing of the rock behind the surface in area (C). This phenomenon seems to be associated with the moisture present in the rock and heat buildup which causes fracturing as the rock is heated up. For actual tunneling operations the underground rock would be expected to be saturated with moisture and the kerfs deeper than in most of the work reported here. Thus, the rock would be subjected to more heat and the associated spalling and cracking due to the cutting operation would be maximum.

The cuts performed on St. Cloud granodiorite produced identical contours to those on Concord gray granite. The slag was of a slightly different color and since the granodiorite had been kept covered it was subject to less spalling and cracking during the cutting operation; otherwise, the cuts were essentially the same. A comparison of actual test runs is shown in Table I.

A typical cut performed on the Dresser basalt is shown in Figure 13 (with rendition as Figure 14). This material cut the easiest of the rocks tested. The front of the cut at (A) on Figure 14 was the most vertical of any of the cuts produced and the side of the cut at (B) tapered out slightly but showed no spalling. There was some spalling at the outside at (C) and (D) but this was significantly less than that experienced with granite because of the reduced quartz content.

As might be anticipated by those knowledgeable in the physical properties of rocks, the cutting experience on quartzite represented the other end of the spectrum from the basalt. During the first cutting tests (at the same cutting speed used on other materials, 3 inch/min.) the plasma produced some spalling before it actually encountered the rock and then melted a small pocket at the top of the rock. This deflected the arc column backwards and caused extinguishment due to high arc voltage. A second cut at slightly slower speed produced considerable spalling and the debris tended to collect at the top of the graphite anode - generating an insulator which again severed the arc column. During a third cut, at still

slower cutting speed, all material removal was produced by spalling and the cutting occurred at a reasonable rate (2 inch/min.) but eventually a large piece spalled off the bottom of the cut and broke the arc column, causing extinguishment. Thus, it is seen that the characteristic high viscosity of the high silica quartzite plus the low heat transfer combined to make quartzite quite difficult to cut. It is interesting to note that each of the efforts to cut quartzite resulted in a crack severing the slab in the plane of the cut. The quartzite is the most easily fractured by localized application of heat and it may well be that this mode may assist in producing satisfactory cutting speeds in this material.

As part of a preliminary screening investigation of arc cutting effectiveness, efforts were made to cut rock with water flowing over its surface and to cut with a significant gap or fissure in the rock. During the cut with moisture the front edge of the rock was tilted at 30° and a sheet of water roughly 4 inches wide and 1/16 inch thick was directed over the inclined face. The presence of the water did not affect cutting speed or performance significantly; thus, it appears that the presence of water does not represent a real obstacle to transferred arc rock cutting.

Two different runs were made with a gap between two granite slabs, one 2 inches thick on top, and a second 6 inches thick. During the first cut the gap was approximately 1/8 inch and the two mating rock surfaces were large enough to represent a significant restriction to air aspiration into the cut. In this case the gap had no effect on cutting. During the second test, however, the gap was widened to 1/4 inch. In this case there was ample room for air to be aspirated into the cut region, or for the hot gas to be deflected into the crack. The cut progressed nicely through the upper piece but the lower rock showed almost no penetration. Certainly this type of configuration, with a gap in the rock face open to the atmosphere, would not be typical of tunneling operations.

Once a satisfactory electrode configuration and gas flow have been established for the transferred arc cutting, the two primary variables are cutting speed and power. Successful cutting has been achieved in the range of 2-1/2 to 12 inches/min., depending on the rock type and thickness. For cutting on very thick rock a slow cutting speed is required to provide sufficient heating (in the lower regions of the kerf) to permit it to wash out. When the

cutting speed is increased (at constant power) the taper at the bottom of the cut increases.

The only type of heat balance that can be run on the transferred arc portion of the cutting operation is what might be called an effective heat balance. This is approached in two different ways; one, by measuring the weight of material removed during a particular cut, and the other by measuring the volume of the kerf region. When this was done for one of the Concord gray granite cuts, approximately 70 cubic inches of material was removed during a 106 second cut at 220 kW. Using a weight of 170 pounds per cubic foot, the energy required to melt the material removed would be 48 kW, based on the heat of melting 380 cal/g (7). This power, divided by the 220 kW applied, gives an effective efficiency of 22 percent. Several other runs produced effective efficiencies in the range of 17-25 percent. It was expected that deeper cuts in the tunneling mode where the hot gas is constrained in the kerf for a longer period of time will be more efficient in extracting energy from the hot gas stream.

Much of the data collected was generated during optimization test series. The best run points from this work are presented in Table I and Figures 15, 16, 17 and 18. Figure 15 shows the variation of cutting speed with arc power at constant rock sample thickness, gas flow and torch geometry. The plot indicates the maximum cutting speed which can be achieved at a given power. Visualize a cutting jet (3 inch sample thickness) of constant velocity and heat flux for the entire depth of the cut. Thus, the bottom of the cut would see the same heat flux as the top. Under these conditions cutting stops abruptly as the cutting speed is increased beyond those values on Figure 15. This curve, thus, shows the ultimate speed at which a plasma of this type (and specific power density) can cut rock. One might speculate that the melt thickness at the bottom of the cut would be greater than at the top, however, it was observed that the momentum of the jet and the characteristics of the molten rock were such that little change in melt thickness occurred in this region.

It is impossible to maintain the power density* constant during such a series of tests since the only way the

*Power density as used here is the energy rate density which the cut face sees and which leads to cutting action.

torch power can be increased with constant gas type and arc length is to increase amperage. This increases power density in the arc and thus that directed on the rock surface; for example, the power density at 400 kW is about 3×10^{-4} kW/m² from interpolation of data and previous measurements by the authors. Experimental data indicates the heat flux increases four times when increasing the power level by four. If the power density were kept constant the cutting speed should have also remained constant, thus, Figure 15 actually depicts the variation of cutting speed with power density (which is synonymous with arc power) for the specific apparatus used.

Figure 18 presents calculated data on the variation of cutting speed with power density. The development of this theory is presented in Appendix A along with a comparison of other heat sources. The theory assumes a melting rock surface with constant liquid film thickness subjected to a fixed power density. This data was developed using best values for thermal conductivity, heat capacity, density, melting point and emissivity of the melt. It appears that this is a rigorous treatment of the cutting phenomenon but its application is limited by the difficulty of experimentally measuring power density and melt thickness.

Visual studies of the granite melting process with both regular and high speed movies shows that the molten rock film in front of the progressing arc is not smooth and uniform, but rather webbish in appearance, with an estimated 20 percent of the surface covered by visible molten rock and the remainder covered by a transparent extremely thin film. This coalescence of material into net-like ridges was probably caused by the high surface tension of the molten rock. Inspection of the cut face after cooling shows this same phenomenon with the webs approximately 1-1.5 mm thick with the intervening area covered by no detectable molten material. If the theoretical curves can be assumed to represent the effect of melt thickness on cutting speed, the average melt thickness measured would appear to agree well with the upper curves on Figure 19. The web nature of the melt surface is shown in Figure 20. It should be noted that the data points plotted on Figure 18 for granite would indicate the melt thickness during cutting is somewhere between 0.1 and 0.2 mm.

It is significant to note that quartzite did not exhibit the surface tension coalescence characteristic of granite. When the quartzite was subjected to the same power density a film in the range of 3-5 mm developed and this prevented cutting at any measurable speed. It appears that the other constituents in the granite tested altered the viscosity characteristics of the melt enough to produce the unexpected phenomena and, thus, reduction in melt thickness to the point where relatively high cutting speeds could be achieved. In the cuts on basalt, very little residual molten material remained on the leading edge of the cut upon shutdown (isolated droplets covering 5-10% of the surface). If one were to speculate on cutting performance of this material on the basis of this knowledge he would predict higher cutting speeds when compared with granite, and this was the case, as indicated on Figure 15. Obviously, a thin molten film must have existed during the cutting process, however, basalt's high fluidity at its melting point appeared to permit the liquid to be washed away rapidly as it was generated, maintaining the film at an extremely thin level.

The data on Figure 18 was generated using a 0.172 inch diameter orifice in the plasma torch. From practical experience, the maximum amperage which can be safely conducted through this diameter, using current cooling technology, is in the range of 600 amperes. The highest power density points generated were produced at 650 amps. This means that further increases in power density and, thus, cutting speed, could not be expected with this device as tested using nitrogen. The curve, however, is extrapolated to 16 inches/min. This higher range of cutting speeds could be reached if: (1) power density in the arc was increased by improving nozzle cooling, or (2) more simply, by increasing the voltage gradient in the arc by selection of different gases such as hydrogen. (Higher voltage gradients indicate higher arc resistivity and, thus, increased power generation per inch of length.) A side effect of such an increased resistivity would be the constriction of the arc diameter at a given power. This should result in a narrower kerf and, thus, more effective use of the power.

Figure 16 shows the minimum power required to produce a vertical cut through a given thickness of granite. (It should be noted that deeper cuts can be made with a lagging cut.) The plasma torch was operated at chamber pressures in the range of 10 to 30 psig. In this pressure range a characteristic jet length of relatively constant heat flux can be attached to each power. This jet length increases as the power rises. Mixing with the surrounding atmosphere breaks up the jet rapidly, in the cutting process this visually results in reduced melting and a lagging kerf. Thus, when running at 40 kW one can observe that the bottom of the kerf begins to lag after a vertical penetration of approximately 1 inch while at 400 kW vertical penetration is in the range of 5-6 inches. Although 1,000 kW has not been run in these tests, prior experience would indicate that a jet length in the range of 12-18 inches could be expected. We suspect, then, that there is adequate power available to permit thicker cutting than that shown on Figure 16, thus, the thickness limitation at a given power is more influenced by the phenomena occurring in the tailflame of the plasma where mixing and diffusion control, i.e. the tailflame should be kept more columniated. We would suspect that improvements in efficiency could be obtained with modifications that would reduce jet mixing, such as, shrouding the plasma with a coaxial sheath of less dense gas which would reduce shear forces, and shaping of the plasma nozzle to produce a more directional flow. The voltage gradient in the arc is approximately 35 volts per inch, therefore, each 3 inches of arc cut thickness requires an additional 100 kW of power. The points on Figure 16 approximately follow this slope. Thus, the slope of the curve appears to be controlled by the electrical characteristics of the system. A variety of anode positions were used, as indicated in Figure 4. As a generalization, maximum cutting takes place between the two electrodes and the second electrode should be located within 2 inches of the jet breakup point.

Figure 17 is a compilation of data points at 240 kW using the angled (Figures 4 (C) and 8) configuration on both Concord gray granite and basalt. As the speed of the cutting device is increased on a given sample the cut gets shallower and finally reaches a point where the device moves so rapidly over the surface that no heat affection occurs. In the case of granite, this is preceded by a region of spalling (since the authors have observed that granite spalls at approximately 1100°F) while with

basalt the transition is more dramatic. At very low speeds spalling becomes the dominant mode of cutting in the case of granite since a large cavity is developed and only the low temperature periphery of the flame contacts the rock. The relative difference between granite and basalt can be explained on the basis of the melting energy requirements, however, the difference in shape of the two curves was not expected.

The tunneling concept proposed prior to awarding of this contract involved the creation of deep narrow kerfs in a tunnel face to relieve 4 foot square blocks attached only at the rear. These blocks, in turn, were to be fractured by the use of dielectric heating to produce thermal inclusions. The dielectric energy was to be coupled into the rock via plasma contacts on two opposing kerf faces. It became obvious early in the program that the practical distance between contacts was too great to permit generation of deep thermal inclusions - only superficial surface heating resulted with one or two through cracks developing. At about the same point in the investigation it was noted that major rock fracturing occurred due to heat buildup in the rock during the cutting process, from observation it was rapidly concluded that cracking from this process would probably be adequate to remove all the intervening rock. Because of the man hours allotted to the program it was agreed, with contract manager approval, that major emphasis be directed to the cutting phases of the program.

PROJECTED TUNNELING PERFORMANCE

The Rapid Excavation Report by the National Academy of Sciences (9) sets as hard rock tunnel goals a 200-300 percent increase in the sustained rate of advance with maximum current capability of about 75 ft/day in 8'-9' tunnels (10). It is the purpose of the following section to propose that plasma cutting could achieve and exceed the goals set out by the Rapid Excavation Committee within a practical power level and the present state of the art of plasma generators.

The data generated on this program has been extrapolated to higher powers utilizing reasonable cut widths (2") and cut depths (24"). These projections, along with National Academy of Science goals, are presented in Figure 21. One typical calculation will be made to demonstrate how the curve was generated.

Assumptions:

- 1) Granite rock @ 200 lbs/ft.³
- 2) 0.48 kWh/lb. required to remove all materials in kerf
- 3) Kerf 2" wide x 24" deep
- 4) Tunnel cross section 8' x 8'
- 5) Cores after cutting are 4' square, i.e. 48' of cut required on each fresh tunnel face
- 6) Cutting occurs 40 minutes of each hour (66% efficient)

Volume of kerf cut on each fresh tunnel face:

$$v = \text{width} \times \text{depth} \times \text{length of cut}$$

$$v = 2/12 \times 2 \times 48 = 16 \text{ ft.}^3 \text{ or } 3200 \text{ lbs.}$$

The power (p) required to melt the above kerf in one hour is

$$p = \text{melting energy} \times \text{lbs. rock melted}$$

$$p = 0.48 \text{ kWh/lb.} \times 3200 \text{ lbs/hr.} = 1536 \text{ kW.}$$

If six 1536 kW torches are used simultaneously it takes 10 minutes to make all the cuts on a new face; this gives a torch speed of 9.6 in/min. (a reasonable speed by extrapolation of data). It was assumed that cutting can be accomplished during two-thirds of each hour, or four cuts can be performed each hour, i.e. 96 cuts per day. Since each cut is 2 ft. deep, the tunnel advance per day is 192 feet.

It is expected that the technology when fully developed could reach or exceed this performance. Dielectric fracturing with the frequencies and electrodes used in this program showed little promise of augmenting the rock removal process; Appendix C is a summary of data, analysis and observations. On the positive side, it appears that the thermal energy imparted to the rock during the kerf cutting process will be adequate to remove the major part of the remaining rock (Figure 22). This removal is expected to provide adequate room for subsequent cutting operations and tunnel advancement.

CONCLUSIONS

The conclusions that can be drawn from the program are as follows:

1. A reliable 400 kW d.c. transferred arc cutting operation has been established which is successful in cutting all of the rock types tested to date (except quartzite) at speeds in the range of 2-12 inches/min. at thicknesses up to 19 inches.

2. It appears that significant rock fracturing will occur during the kerf cutting process due to heat buildup in the rock in most rock types tested.

3. An electrode geometry has been tested which permits continuous cutting on a simulated vertical tunnel wall at depths up to 12" and speeds in the range of 2.5-4 inches/min. and continuous cutting at depths beyond 19" if more ideal laboratory geometries can be used.

4. The concept of producing thermal inclusions in rocks for fragmentation by using either mechanical or plasma electrical contacts to the surface does not appear to be practical. Only surface heating and limited cracking occurred.

5. The data generated appears to indicate higher cutting speeds and deeper cuts can be achieved with higher powers and arc power densities.

6. Extrapolation of the cutting data to 9,000 kW indicates tunneling speeds of 200 ft/day could be expected with an 8' tunnel.

PATENTS AND INVENTIONS

No inventions were made during this contract.

APPENDIX A

THEORETICAL CONSIDERATIONS, COMMENTS ON OTHER
HEAT SOURCES AND ENERGETICS AND SPEED OF CUTTING

by

Mark P. Freeman, Ph.D.

HEAT REQUIREMENTS FOR ROCK MELTING

Cutting the kerf involves straightforward melting of the rock at the surface (or melt/rock interface) because of the temperature rise related to the heat flow into the rock. The general problem of heat conduction with melting is not well developed (11). However, without specifying the heat source for the moment, we can evaluate the energetics of the process from the rock material properties by assuming (a) a steady state thickness of melt, and (b) a steady state temperature profile relative to the melt interface. Such an analysis is carried out below.

The relevant material properties for rocks are not well known in that they vary widely depending on the source. However, for the present discussion reasonable values of these properties have been chosen for three rocks of pragmatic interest and are given in Table II. Cutting velocities for these various rocks are shown in Figure 23 as functions of the net heat actually transported into the rock. The rather trivial discrepancy in cutting speeds only reflects the difference in physical constants of the rock. The disparity becomes much greater if we include radiation loss from the surface of the melt. In Figure 19 we plot cutting speed for charcoal granite vs. heat flux convected to the surface of the now radiating melt for various thicknesses of melt. In Figure 24 we compare again the various kinds of rock assuming a uniform thickness of melt.

Two things become immediately clear from this simple analysis. First, the heat flux required to cut charcoal granite at the rate of, say 12 in/min. ($\approx 0.6 \times 10^8$ W/m²) even for a 100 μ melt thickness, is in a range that excludes most conventional methods of directing heat to surfaces (this may readily be seen from Table III where various devices are intercompared) (12). This is as opposed to Dresser basalt on the one hand which may, in fact, be cut with a sufficiently hot knife and to sandstone on the other, the cutting rate of which will probably be limited by vaporization. (Fortunately, ultra-refractory rocks like sandstone are sufficiently soft that they may easily be removed by mechanical techniques.)

Second, for a finite heat flux, thickness of melt can spell the difference between success and failure for a particular device. For some rocks, economical melting,

regardless of the method, may require fluxing of the melt so as to reduce its viscosity to a value that permits gravity drainage and/or air blast removal.

HEAT SOURCES SUITABLE FOR HARD ROCK CUTTING

Returning now to Table III, we single out those directed heating processes capable of melting, say, charcoal granite at a finite rate;

- a) Laser heating
- b) Electron beams
- c) Heated solid bodies
- d) Electric arcs.

Laser Heating

Although ideally suited to the work in many ways, current technology of cw lasers limits the total amount of power available to about 150 kW and that only for at most minutes at a time. The top heat flux of 10 MW/m^2 is less than satisfactory. However, focusing can improve the figure substantially but at the cost of depth of field. If the duty cycle problem can be solved and, depending on the extent of attenuation of the beam by the vaporizing material, this method could well one day be practicable. However, it is our understanding that, based on an overview of current technology, this line of development is not regarded as promising at present.

Pulsed lasers have the requisite energy density but at the present state of development lack the average power requirement. This approach seems less likely to succeed than that of the cw laser.

Electron Beam

One technique for melting deep kerfs in rock is utilization of an electron beam (13). It would appear that initial experiments in this area have uncovered certain technological problems which will limit the application of this heat source. Initial experiments have demonstrated beam defocusing which limits penetration into the rock.

In addition, the vapors produced during the vaporization process limit the ability of the beam to penetrate into the kerf. In addition, the process requires extremely high voltage (100,000 V), sophisticated vacuum equipment, and will generate x-rays.

Heated Solid Body

Cutting with heated solid bodies (the hot knife concept) is really somewhat beyond the state of the art at the stated heat flux, but is included because one has the possibility here of containing the radiation and, thus, dramatically improving the efficacy of the device (i.e. use Figure 23 instead of 19). Even so, it is clearly sub-marginal for charcoal granite. It is believed that, again, at the temperatures required for anything higher melting than basalt, materials of construction will be the limiting factor.

Electric Arc

Theory - Before turning our attention to ways in which surfaces may be melted by electric arc, it is well to briefly review the principles of electric arc operation (14, 15).

The ionization on which an arc depends for its electrical conductivity comes from the higher temperature (10,000-20,000°K), partial dissociation of atoms into electrons and positive nuclei according to the well understood principles of chemical equilibrium. Now the arc is some complex of individually well understood processes, ionization, recombination, joule heating, heat conduction and heat convection due on the one hand to anisotropic magnetic pressures with consequent high velocity streaming, and on the other hand to buoyancy effects due to density gradients. Buoyancy effects, by the way, are surprisingly important for free arcs. [Trivially, for a horizontal arc they cause the arc to bow upward in the middle (hence, the name arc). More importantly, Steenbeck (16) has shown that in free fall (zero gravity), where there are no buoyancy caused currents, an arc will expand to fill its container (at the same time becoming much cooler).] If all the known processes are mathematically modeled and the thus highly coupled differential equations

solved, it is found that they are determinate in such things as arc power per unit length, conductance, and arc radius (17). For the development of intuitive thinking, however, it is probably better to lean on the laws of irreversible thermodynamics, a procedure that has been shown to give identical results starting from a much lower level of information (17). Specifically, for arcs, the second law is equivalent to saying that in general, all else equal, an arc will spontaneously assume that configuration minimizing its electric field.

When an arc constrained to a constant current is confined or contacted by a close fitting material (and thus necessarily "cold") wall, cooling of the arc boundary is thus much stronger and the arc defined by its temperature isopleths shrinks. To maintain its current with a smaller cross section, it must operate with a higher field. In the process, it spontaneously becomes much hotter and more highly ionized and the power dissipated per unit length (and, hence, by energy balance the heat flux to the surrounding walls) can go up by as much as an order of magnitude over the value for the free arc. Note that the radial temperature profiles can assume a quite non-intuitive shape [e.g. Figure 25 (18)] because of the strongly variable material properties of the arc fluid caused by various ionization and atomic dissociation phenomena at different temperatures.

Directing the Arc Heat Onto a Surface - Although the heat generation of an arc is adequate to the task, the number of ways in which its heat may be directed into a kerf are limited.

The d.c. or a.c. plasma jets (19) are probably inappropriate for deep penetration because the formation of a satisfactory steady state cutting profile is precluded by attenuation of the free jets due to conduction to the surfaces and to entrainment of cold ambient gases and vapor (although coanda effect attachment to the rock face might be expected to cause the jet to persist longer than might otherwise be expected).

Directing the arc into the rock by means of a magnetic field is a possibility, but dispersal of the molten rock becomes a problem. This suggests blowing the arc into the fissure so that the gas convecting the arc into the fissure can serve the second purpose of cleaning out the "magma" as well.

In particular, the concept investigated in this program weds the concept of the plasma jet and the blown arc represented by the so-called transferred arc (20). Here the plasma jet is heated by an arc burning external to the jet device. This means on the one hand that the arc will be attached to the surface (coanda effect) and that the magma will be blown from the fissure while, on the other hand, any part of the cut that "lags behind" will cause a "constriction" of the arc (i.e. its temperature isopleths will be more tightly bunched) with consequent increase in heat flux. Thus, a steady state cut is assured. It is exactly this simple configuration that has been found by TAFA to be highly successful in melting rock. As mentioned above, a very high fraction of the energy dissipated in the arc goes into cutting the rock and even at the current state of development it will cut 6" thick granite at the rate of 3 in/min. Its curved configuration and the fact that it can produce a moving cut of constant shape in a rock face suggest referring to it as an arc plasma saw.

ENERGETICS AND SPEED OF CUTTING

Glossary

- A = Area of rock
- c = Heat capacity per unit mass of solid rock
- L = Heat of liquifaction of rock
- K = Thermal conductivity
- T = Temperature
- T_m = Melting temperature of rock
- T_s = Surface temperature of melt
- T_0 = Initial rock temperature
- t = Time
- U = Cutting speed

W = Heat flow

x = Position

ϵ = Emissivity

κ = Group of constant used in derivation

ρ = Density of solid rock

σ = Stefan-Boltzmann constant

Subscript 2 = Refers to melt

Summary

For rock cutting in steady state it is found convenient to introduce a transformed cutting rate U^1 . It may be immediately identified with the heat flux into the surface of the melt and is directly proportional, related through use of material properties, to the true cutting rate, U:

$$U^1 = U \cdot \rho c [(T_m - T_0) + L/c] \quad (a)$$

The total power that must be transferred to unit area of the surface of the rock to achieve a given transformed velocity U^1 is just

$$W_T/A = U^1 + \epsilon \sigma T_m^4 \left[1 + \frac{\delta U^1}{K_2 T_m} \right]^4 \quad (b)$$

In the limit of thin fluid melt layers this may be rearranged to give U^1 as a function of heat flux:

$$U^1 \approx \frac{W_T/A - \epsilon \sigma T_m^4}{1 + \frac{4 \delta \epsilon \sigma T_m^3}{K_2}} \quad (c)$$

Finally, in the case of a viscous melt vaporization imposes a limit on cutting speed and in this case we find a limiting speed of

$$U^I \Big|_{\max} = \frac{K_2}{\delta} (T_b - T_m) \quad (d)$$

and a maximum productive heat flux of

$$W_T/A \Big|_{\max} = \frac{K_2}{\delta} (T_b - T_m) + \epsilon \sigma T_b^4 \quad (e)$$

Recommendations

To make proper use of these equations they should be numerically evaluated for rocks of interest. It would be relatively trivial to insert values of thermal conductivity, heat capacity, heat of liquifaction, density, melting point and emissivity of the melt to generate a family of curves of heat flux vs. cutting rate for various thicknesses of melt δ . Similarly it would be equally straightforward to compute and plot limiting cutting rates vs. limiting production heat fluxes for different melt thicknesses of the different rocks of interest. Given the material properties listed above a satisfactory numerical analysis should require no more than eight hours including reporting the results.

Theory

The Solid Rock - Consider a semi-infinite solid moving at velocity U toward the left. The plane $x = 0$ is maintained at T_m . (We thus model a uniform melting surface with the coordinate origin fixed in the plane of melting.)

$$\begin{array}{lcl} \text{Heat flux} & \rightarrow & U \leftarrow \\ = K \frac{\partial T}{\partial x} \Big|_{x=0} & \rightarrow & T + dT = T(x + Udt, t + dt) \quad (1) \\ & \rightarrow & \text{or} \\ & \rightarrow & T + dT = T + U \frac{\partial T}{\partial x} dt + \frac{\partial T}{\partial t} dt + \dots (2) \end{array}$$

We now assume the solid is moving (i.e. the surface is melting) in such a way that a steady state exists in our coordinate system. That is,

$$\frac{\partial T}{\partial t} = 0 \quad (3)$$

$$\text{Now } \frac{dT}{dt} = -\frac{K}{\rho c} \frac{\partial^2 T}{\partial x^2} = -\kappa \frac{\partial^2 T}{\partial x^2} \quad (4)$$

where ρ is the rock density and c its heat capacity. κ is defined by Eq. (4). Introducing (3) and (4) in (2) we get

$$\kappa \frac{\partial^2 T}{\partial x^2} = -U \frac{\partial T}{\partial x} \quad (5)$$

The solution of which is just

$$\frac{T - T_0}{T_m - T_0} = \exp \left\{ -\frac{U}{\kappa} x \right\} \quad (6)$$

where T_0 is the initial rock temperature and the conditions have been used:

$$\begin{aligned} \text{as } x \rightarrow \infty, T &= T_0 \\ \text{as } x \rightarrow 0, T &= T_m \end{aligned} \quad (7)$$

By differentiation of (6)

$$\kappa \left. \frac{\partial T}{\partial x} \right|_{x=0} = \frac{K}{\rho c} \left. \frac{\partial T}{\partial x} \right|_{x=0} = -U(T_m - T_0)$$

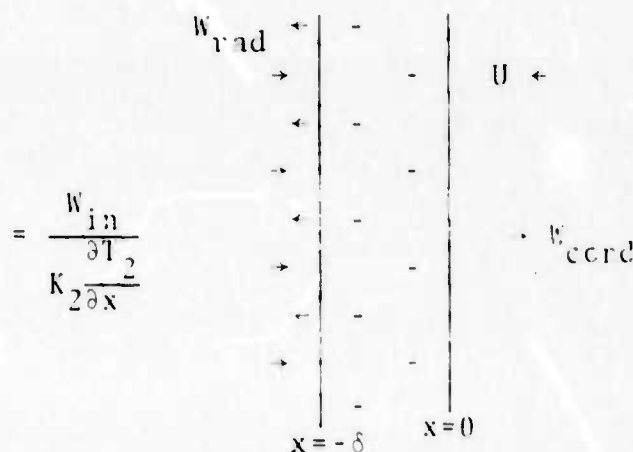
or

$$\frac{W}{A} = -U \rho c (T_m - T_0) \quad (8)$$

where W/A is the power transferred to unit area of the rock. Equation (8) simply says that cutting speed is directly proportional to rate of heat transfer per unit area which is not unexpected. Expected also is that for a given available power the cutting speed is inversely proportional to volumetric heat capacity and to the temperature rise required for melting. Up to this point we have only considered heat conducted away into the rock. We thus summarize.

$$U = \frac{W_{\text{cond}}}{A \rho c (T_m - T_0)}. \quad (9)$$

The Melt - We now consider processes to the left of the plane of melting, specifically the melt, assumed to have a constant thickness δ determined by viscosity, gravity, and jet shear forces.



Denote the liquid phase by the subscript 2. Then:

$$\frac{W_{\text{cond}}}{A} = K_2 \left. \frac{\partial T_2}{\partial x} \right|_{x=0} - U L \rho \quad (10)$$

liquifaction per gram.

We now assume the melt is opaque so that

$$K_2 \left. \frac{\partial T_2}{\partial x} \right|_{x=0} = K_2 \left. \frac{\partial T_2}{\partial x} \right|_{x=-\delta} \quad (11)$$

or if $T_2 = T_s$ at $x = -\delta$

$$K_2 (T_s - T_m) = K_2 \left. \frac{\partial T_2}{\partial x} \right|_{x=0} \delta \quad (12)$$

Substituting from (12) in (10) we get

$$\frac{W_{\text{cond}}}{A} + UL\rho = \frac{K_2 (T_s - T_m)}{\delta} \quad (13)$$

Introducing (9) and solving for U:

$$U = \frac{1}{\delta} \frac{K_2}{\rho c} \frac{(T_s - T_m)}{[(T_m - T_0) + L/c]} \quad (14)$$

Equation (14) suggests defining a transformed cutting speed that internalizes the material properties of the rock.

$$U^1 = \frac{K_2}{\delta} (T_s - T_m) = \frac{W_{\text{in}}}{A} \quad (15)$$

where

$$U^1 = U \cdot \rho c [(T_m - T_0) + L/c] \quad (16)$$

The material property K_2 has not been included in the definition of U^1 because K_2 and δ are almost certainly affected by fluxing the melt for lower viscosity. It is of course possible that the melting temperature could also be reduced, but we use this abbreviation anyway as it is only a matter of convenience and does not serve as a base for approximation. Note that the units of U^1 are $\text{cal}/\text{cm}^2/\text{sec}$.

For low melting materials, the cutting speed is given by (15) by setting T_s equal to the boiling point of the rock, T_b . The (transformed) velocity then depends only on the thermal conductivity and inversely on the liquid layer thickness. However, radiation is appreciable when most rocks melt. We write:

$$W_T = W_{in} + W_{rad} \quad (17)$$

$$W_T/A = U^1 + \epsilon \sigma T_s^4 \quad (18)$$

where ϵ is the emissivity and σ the Stefan-Boltzmann constant. We substitute for T_s from (15)

$$\frac{W_T}{A} = U^1 + \epsilon \sigma T_m^4 \left(1 + \frac{\delta U^1}{K_2 T_m}\right)^4 \quad (19)$$

Neglecting vaporization, this expression relates the transformed cutting speed to the power requirement. If in addition we assume that $(T_s - T_m) \ll T_m$, Equation (19) may readily be inverted:

$$U^1 = \frac{W_T/A - \epsilon \sigma T_m^4}{1 + \frac{4 \delta \epsilon \sigma T_m^3}{K_2}} \quad (20)$$

Note that the effect of vaporization will actually be to put an upper limit on T_s . Thereafter additional heat will serve only to boil away rock which decreases heat transfer to the melt and is such an energetically unfavorable process that it contributes inconsequentially to the cutting rate. However, this does give us an expression for maximum cutting rate ($T_s = T_b$ in Equation (15)) and the power required to achieve that rate (Equation 18).

$$U^1|_{\max} = \frac{K_2}{\delta} (T_b - T_m) \quad (21)$$

and

$$W_T/A|_{\max} = \frac{K_2}{\delta} (T_b - T_m) + \epsilon \sigma T_b^4 \quad (22)$$

It is doubtful if the maximum could be achieved for rock with a very fluid melt by use of any known arc device, however, for those with viscous melt it may well be the limiting factor in rock cutting.

Note that we have considered in W_T only the heat transferred directly to the melt. Arc power will generally be quite a bit higher at least half of it being lost in non-productive heat transfer to the walls of the kerf. No attempt is made to analyze that factor at this time.

APPENDIX B

BACKGROUND, INTERNAL HEATING TO CREATE
THERMAL INCLUSIONS VIA DIELECTRIC MEANS

The concept here is to fragment rock by creating a thermal inclusion via dielectric means. Experiments are described in detail (5). The use of surface contact electrodes on asbestos, rock salt, granite and labradorite has been described (22). External electrodes appear to present an advantage in ease of application of power, however, the location and size of the thermal inclusion is less easily controlled and would undoubtedly vary more widely with rock properties and imperfections. It is interesting to note, however, that even with these limitations, fracturing powers of 12 kWh/m³ were obtained (22) via external electrodes on less heterogeneous rocks as compared with 3.5 to 5 kWh/m³ with insert electrodes (21).

Figure 3 of Reference 22 indicates the effect of field strength (volts per centimeter) on crushing time for various rock samples. These data have been replotted as Figure 26. The data point out that higher field strengths can decrease crushing times considerably. Thirumalai (5) indicates that to avoid arc breakdown of the thermal inclusion one should keep rock voltage gradients below 3,000 volts per centimeter. From Figure 26 it appears that increasing voltage gradients up to 600 v/cm reduces cracking time considerably with no data above this.

Dielectric heating of a material can be expressed in the following way (23).

$$\text{Watts/cm}^3 = 0.555 \times D_C \times D_F \times f \times V^2$$

where

D_C = dielectric constant

D_F = dissipation factor

f = current frequency (MHz)

V = voltage gradient impressed on rock (kV/cm)

It should be noted that both D_C and D_F are properties of the rock. In any experimental program it is important that one optimize the process with the variables under his control. D_C and D_F are expected to vary with temperature. Figure 27 (Reference 24) shows the variation of these two

parameters with temperature for fused silica. Because of the wide variation in D_F and D_C in the temperature range of interest, care should be devoted during the program to measuring the effect of these variations on power supply-load coupling, and the magnitude of corrective tuning during loading to achieve maximum performance, i.e. if the effect of varying loss factor is great, capacitance might have to be added during the heat up cycle to maintain a constant tank circuit impedance.

It can also be seen from the dielectric heating equation presented that the internal heating is a linear function of frequency. The data reported in Figure 26 was for frequencies in the 3-6 MHz range. Since the TAFE laboratory is equipped with frequencies up to 20 MHz, one might postulate that it could achieve a 3-6 times improvement over the performance indicated in Figure 26 - a significant reduction resulting in cracking in a few seconds. Practical experience in the areas of arcing and equipment maintenance dictates the use of the lowest possible frequencies. At 1,000 kW, for example, 450 KHz is standard for pipe mill welding, and this power range is available on an off-the-shelf basis. Essentially, no unusual power supply maintenance or arcing problems are present in such a system. Similarly, 13 MHz is available at this power range for dielectrically heating plywood; however, more care must be taken to protect components from arcing, especially in undesirable environments containing high humidity and contaminants. This is not to say that the electrical engineering problems are insurmountable, rather that where equivalent performance may be achieved, lower frequencies are recommended; thus, data should be made available over a wide frequency range to assist in future engineering evaluation. The experimental program envisioned would generate data over the range of 450 KHz to 20 MHz.

It should also be obvious from the dielectric heating equation that since heating is a second power function of volts per centimeter, considerable emphasis should be placed on understanding this parameter. Because of well known x-ray generating problems, voltages should be kept below 18,000 to eliminate the need for shielding. On the other hand, Figure 26, previously discussed, points out the importance of increasing this item to reduce crushing time.

It should also be obvious that reduction in heating time to achieve the proper sized thermal inclusion will also reduce conduction losses through the rock and, therefore, further decrease the time required. This was pointed out experimentally by Thirumalai (21) via comparison of rocks of different conductivity (Sioux quartz vs. granite and basalt).

APPENDIX C

SUMMARY OF DIELECTRIC HEATING INVESTIGATIONS

by

John W. Poole

The initial work on dielectric heating was done at about 8 MHz which is the maximum design operating frequency for the standard output circuit on the 100 kW output Lepel unit. The filter circuit used to protect the d.c. power supplies was an improved version of the π filter which was made up several years ago at TAFA. The leads from the d.c. torch to the filter were about 12 feet long. During the early work the ground side of the r.f. circuit was connected to the d.c. torch, and the system seemed to work quite well for rocks up to four inches thick.

To establish a frame of reference mechanical electrodes were first attached to 8-10 inch thick rock to attempt heating and cracking. No heating could be produced at the ground potential electrode and this led to studies with the plasma torch in the high voltage lead rather than ground lead (Figure 6). Additional tests demonstrated that one could not generate a crack in thick rock with the d.c. laminar flame heating only. Thus, it was concluded that the laboratory setup should be modified to couple the high r.f. potential directly to the d.c. plasma.

Attempts to operate with the above connection led to severe difficulties with the r.f. oscillator, i.e. recurrent arcing between turns of the grid tuning coil, excessive loading of the tank circuit so that oscillations would stop, and power control difficulties whereby the unit would jump to a maximum power output condition. The problems were solved systematically and eventually led to the following changes.

1. Discard the r.f. filter.
2. Substitute a dual-tuned tank circuit approach (Figure 6) for coupling the r.f. power to the d.c. torch - rather than the direct coupled output circuit (Figure 6).
3. Operate a 5 MHz instead of 8 MHz.
4. Improve the grounding of the oscillator cabinet.
5. Improve the shielding and the grounding of the power control cable to the rectifier cabinet including a capacitor filter network to ground on each lead.

As a result of these changes the r.f. test setup functioned smoothly over a wide range of conditions with complete reliability. Figure 5 (A) shows the test setup in operation.

Approximately 20 fracturing tests were made with the setup [shown in Figure 5 (A)] and the following conclusions can be drawn.

1. Deep cracking cannot be generated by the laminar flame operating by itself.
2. The r.f. voltage can only be turned up to about 7,000 volts peak (5,000 v.r.m.s.) before arc tracks begin to form on the rock surface.
3. Maximum local heat penetration and deep cracking efficiency is achieved at the 7,000 volt point.
4. Turning up the r.f. power to 11,500 volts peak (8,100 v.r.m.s.) resulted in arc tracks about 4" long [Figure 5 (B)]. The track pattern normally has 4 to 6 arcs emanating symmetrically from the laminar plasma foot point.
5. With the r.f. voltage at 11,500 v peak, the top of the rock tends to spall or thin layers separate from the main body of the rock. Deep cracking does not take place.
6. If the r.f. is turned up still higher, the arcs dissipate in the surrounding atmosphere some after traveling four feet.
7. The arc tracks which form about 7,000 v appear to be the same with plasma or solid contacts. Experimental scatter due to different rock strengths, ruff directions, etc., masked differences which might exist.
8. The heat balances indicate:
 - 55% power to oscillator cooling,
 - 15% power to coil,
 - 10% power to calorimeter, and the remaining
 - 20% power to the d.c. torch and the rock

at typical operating conditions. Instrumentation was used to obtain accurate cooling water heat balances, however, no instrumentation was available to measure the dielectric current, voltage, and phase angle directly.

9. The cracking accomplished by dielectric heating generates a fine crack across the smallest cross section of the sample from the hot zone to the edge. Typical sample size has been 8" x 8" x 12". Catastrophic separation was not demonstrated.

10. In comparing our work to Thirumalai (21) we have the distinct disadvantage of working from the surface. His roughly cylindrical thermal inclusion produces shear stresses at the bottom of the heated zone that help break the rock into several pieces.

11. The biggest limitation to this type of heat fracturing from our experience is the surface arcing that takes place at high r.f. voltages. This seems to be aggravated somewhat by the ionized gas already present in the laminar flame, but conversely seems to be helped somewhat by the puddle of molten rock established by the tip of the laminar flame.

12. A statistical analysis was made of 13 runs on the dielectric fracturing setup, 11 using laminar flame contact and two using a solid contact. The correlation was not good on any of the relationships of time, width, height, or volume fractured as a function of peak r.f. volts, r.f. power, and total effective power (r.f. + d.c.). It must be concluded that nothing significant is exhibited by these direct comparisons.

13. Another statistical analysis was based on the hypothesis that the time to cause a crack should be inversely proportional to the r.f. power and the (volts/inch) squared and directly proportional to the minimum dimension of the top face of the rock. The equation is

$$\frac{1}{T} = \frac{1}{K_1} \left(\frac{E}{h}\right)^2 \frac{(r.f. \text{ kW})}{W}$$

or

$$K_1 = T \left(\frac{E}{h}\right)^2 \frac{(r.f. \text{ kW})}{W}$$

The proportionality constant K, gives an indication of the effectiveness of a particular dielectric fracturing test.

This analysis demonstrated no correlation if all of the runs are taken together. However, the runs can be divided into three categories that show close relationships.

a. Moderate r.f. power and voltage (low enough so that no arc tracks form on the rock surface). This shows $\bar{K}_1 = 1.675$ and $V = .02$ where V is the coefficient of variation

$$= \frac{S}{\bar{K}_1} *$$

b. High r.f. power and voltage using the d.c. laminar flame contact. As mentioned elsewhere, this mode of operation produces mostly spalling of the top surface. For this case $\bar{K}_1 = 7.5$ and $V = 0.44$.

c. High r.f. power and voltage using solid metal contact electrodes. There was significant surface arcing and again the tendency to spall the top surface. $\bar{K}_1 = 23.3$ and $V = 0.11$. Thus, the results were uniform but the cracking effectiveness was an order of magnitude poorer than for category 1.

In summary, rock fracturing by applying 5 MHz r.f. energy at the surface to produce thermal inclusion cracking does not appear particularly attractive. Use of the laminar d.c. contact has some attractive features and some detrimental ones, but the overall evaluation would be that it does not strongly enhance what is inherently a poor fracturing technique. The advantage of higher frequency fracturing referred to previously was not demonstrated because of time and apparatus problem limitations.

*S = Standard deviation

\bar{K}_1 = Mean Value of the Constant

BIBLIOGRAPHY

1. Klasson, G. A., "Plasma-Torch Cutting," Mechanical Engineering, (Aug. 1961).
2. Cobine, J. D., "Gaseous Conductors," Dover Publications, New York City, 1958, p. 328.
3. O'Brien, B. L., et al., "Advances in Plasma Arc Cutting," Welding Journal, 43 (12) (1964).
4. Wodtke, C. H., "Constricted-Arc Process Cuts Metal Under Water," Metal Progress (Dec. 1960).
5. Thirumalai, K., "Rock Fragmentation by Creating a Thermal Inclusion with Dielectric Heating," Bureau of Mines RI 7424, 1970.
6. Kohl, W. H., "Materials and Techniques for Electron Tubes," Reinhold Publishing Corp., New York, New York, 1960, p. 20.
7. Thirumalai, K., "Potential of Internal Heating Method for Rock Fragmentation," 12th Symposium on Rock Mechanics, Rolla, Missouri, Nov. 1970.
8. Tuchman, A. and Enos, G., "Experiments to Establish Current Carrying Capacity of Thermionic-Emitting Cathodes," NASA CR-73186, 1967.
9. Rapid Excavation - Significance - Needs - Opportunities, National Academy of Sciences Publication 1690, 1968.
10. Personal communication, Professor E. P. Pfleider, University of Minnesota, and Chairman of "Rapid Excavation" Committee, April 22, 1971.
11. Carslaw, A. S. and Jaeger, J. C., "Conduction of Heat in Solids," Oxford Press, 1947, p. 71.
12. Adapted from a table by T. B. Reed, personal communication.
13. First Quarterly Technical Report, "Use of Electron Beam Gun for Hard Rock Excavation," Westinghouse Electric Corporation, Sunnyvale, California, Apr. 30, 1971.

14. Maecker, H., Z. f. Physik, 157, 1 (1969).
15. Finkelburg, W. and Maecker, H., "Handbuch der Physik," Vol. XXII (Springer verlag, 1962), pp. 259-444.
16. Steenbeck, M., Phys. Z., 33, 809 (1932).
17. Peter, Th., Proceedings Fifth International Conference on Ionization Phenomena in Gases, Munich, 1961 (North Holland Publishing Co., Amsterdam).
18. Maecker, H., Z. Naturforsch, 6, 1102 (1956).
19. Thorpe, Merle L., "The Plasma Jet and Its Uses," Research/Development, Jan. 1960.
20. O'Brien, B. L., Welding J., 43 (12), (1964).
21. Thirumalai, K., "Rock Fragmentation by Creating a Thermal Inclusion with Dielectric Heating, Bureau of Mines RI7424, September 1970.
22. Semenov, V. M., et al., "Crushing of Excessively Large Rocks by Means of High Frequency Current," Building Materials, USSR, Vol. 10, 1964, pp. 9-11.
23. Cohl, W. H., "Materials and Techniques for Electron Tubes," Reinhold Publishing Co., 1960, p. 62.
24. von Hippel, A. R., "Dielectric Materials and Applications," MIT Press, 1954, p. 402.

TABLE I
COMPARATIVE CUTTING PERFORMANCE OF THE ARC PLASMA SAW*

	Slab Thickness	Arc Power (kW)	Cutting Speed (ipm)	Cut Dimensions			
				A	B (in)	C	D
Concord Gray Granite	6	182	3	5-3/4	4-1/4	3/4	4-1/4
	8-1/4	218	2.5	4-3/4	3-3/8	3/4	5
	11-1/4	270	2.5	7-3/8	3-1/2	3/4	6
	13	300	1.8	4-3/4	2-3/4	1	5
	17 ^a	375	2.5	12	2-1/4	1	7
	19 ^a	325	2.5	13-1/4	1-1/4	1	5
St. Cloud Charcoal Granite	26	465	2.5	3	0 ^b	1	9-1/2
	6	193	3	5-1/4	3-1/4	3/4	5
Dresser Basalt	6	220	3	6-3/8	4-7/8	3/4	5
	6-1/4	253	6	7-3/8	2-1/2	5/8	5
Jasper Quartzite	6	275	≈2.5Δ	1-3/4	2-1/2	4	6

* See drawing (right) and code below.

A - Penetration at top of cut

B - Penetration at bottom of cut

C - Width at top of cut

D - Vertical penetration under torch

Δ - Spalling only - no molten product

^aHorizontal arc with anode on opposite side of block.

^bFailed to cut deeper than 17 (vertical arc).

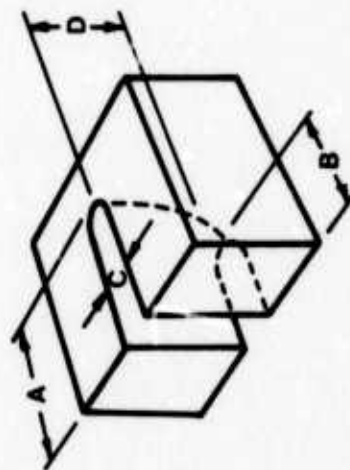


TABLE II
MATERIAL PROPERTIES FOR VARIOUS ROCKS
ENCOUNTERED IN HARD ROCK TUNNELING¹

	Dresser Basalt	Charcoal Granite	Berea Sandstone ²
Density, ρ , kg/m ³	2.97×10^3	2.72×10^3	2.48×10^3
Heat Capacity, c , J/kg ^o K	1.07×10^3	1.11×10^3	1.16×10^3
Melt Temperature, T_m , ^o K	1353 ²	1513	1983
Heat of Liquifaction, L , J/kg	1.57×10^6	1.60×10^6	1.60×10^6
Conductivity, K , watt/m ^o K	1.76	1.32	1.10

¹Unless otherwise noted, properties taken from Table 2, p. 11, Potential of Internal Heating Method for Rock Fragmentation by K. Thirumalai; paper presented at 12th Symposium on Rock Mechanics, Rolla, Mo., Nov. 16-18. 1970.

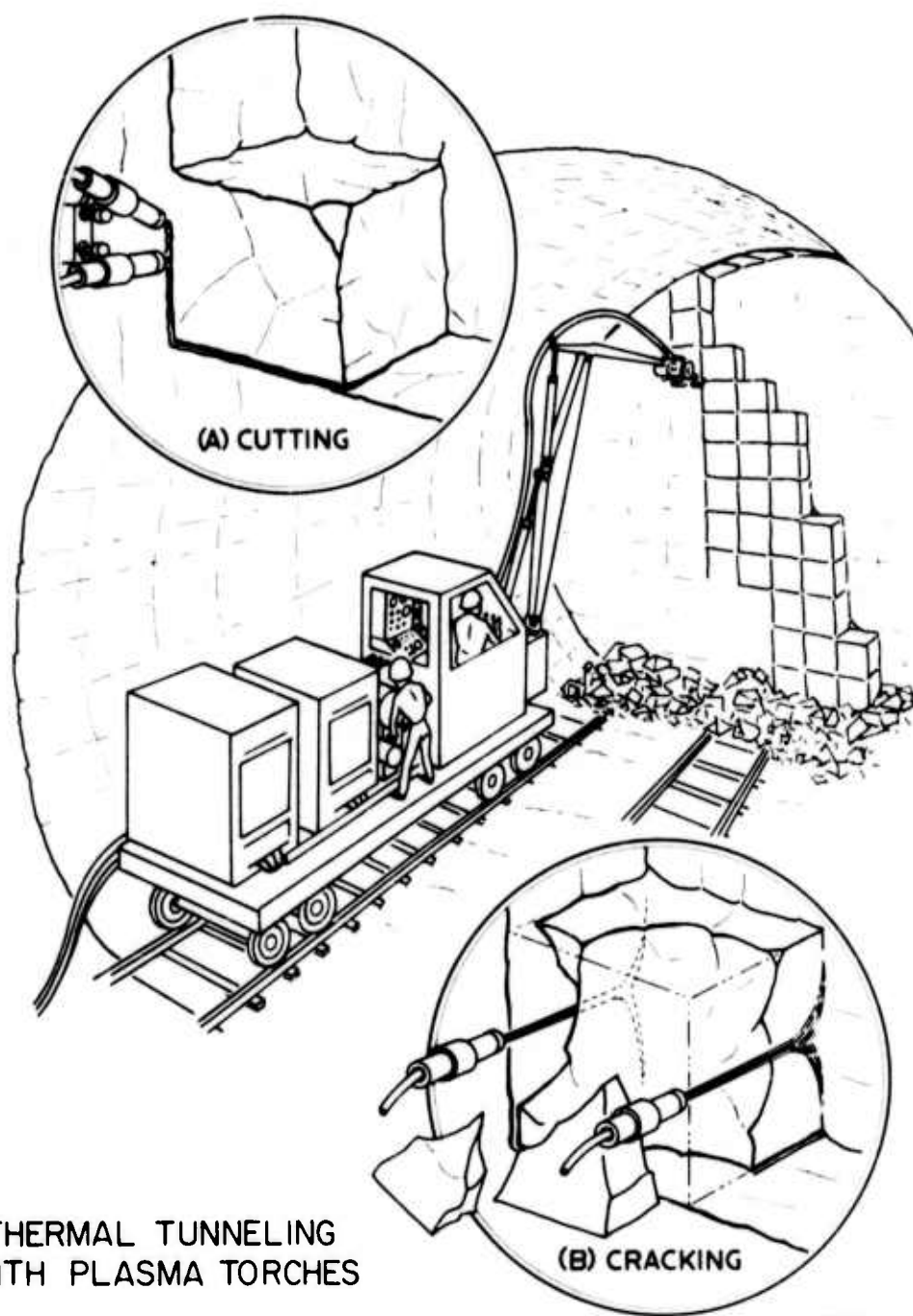
²Estimated

TABLE III
DIRECTED HEAT TRANSFER

Device	Energy Flux Limiting Law	Conditions and Assumptions	Measured or Calculated Heat Flux to Surface (Flux-watts/m ²)
"Soldering Iron"	$E = \kappa \frac{\Delta T}{\Delta X}$	$\kappa = 1.5 \frac{\text{watts}}{\text{cm}^{\circ}\text{C}}$ $\Delta T = 500^{\circ}\text{C}$ $\Delta X = 0.2 \text{ cm}$	0.38×10^8
Open Flame	$E = v h$ v subsonic	$v = 9 \times 10^3 \text{ cm/sec}$ $h = 0.5 \text{ j/cm}^3$ $r = 0.3 \text{ cm}$	0.02×10^8
Constricted Flame	$E = v h$ v sonic	$v = 9.9 \times 10^4 \text{ cm/sec}$ $h = 0.5 \text{ j/cm}^3$ $r = 0.3 \text{ cm}$	0.2×10^8
Constricted Arc (H ₂ Plasma)	$E = v h$ (+ jE if transferred)	$v = 8.5 \times 10^5 \text{ cm/sec}$ $h = 0.75 \text{ j/cm}^3$	2.5×10^8
Open Arc	$E = jE + v h$	$I = 200 \text{ amp}$ $V = 11 \text{ volts}$ $r = 0.3 \text{ cm}$	0.49×10^8
Electron Beam	$E = jV$	$V = 3 \times 10^4 \text{ volts}$ $I = 0.25 \text{ amp}$ $r = 0.04 \text{ cm}$	150×10^8

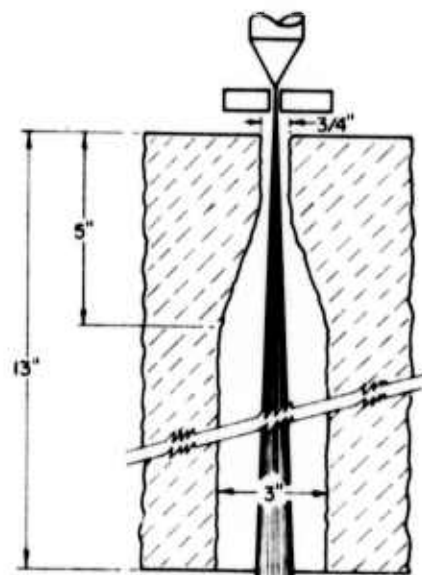
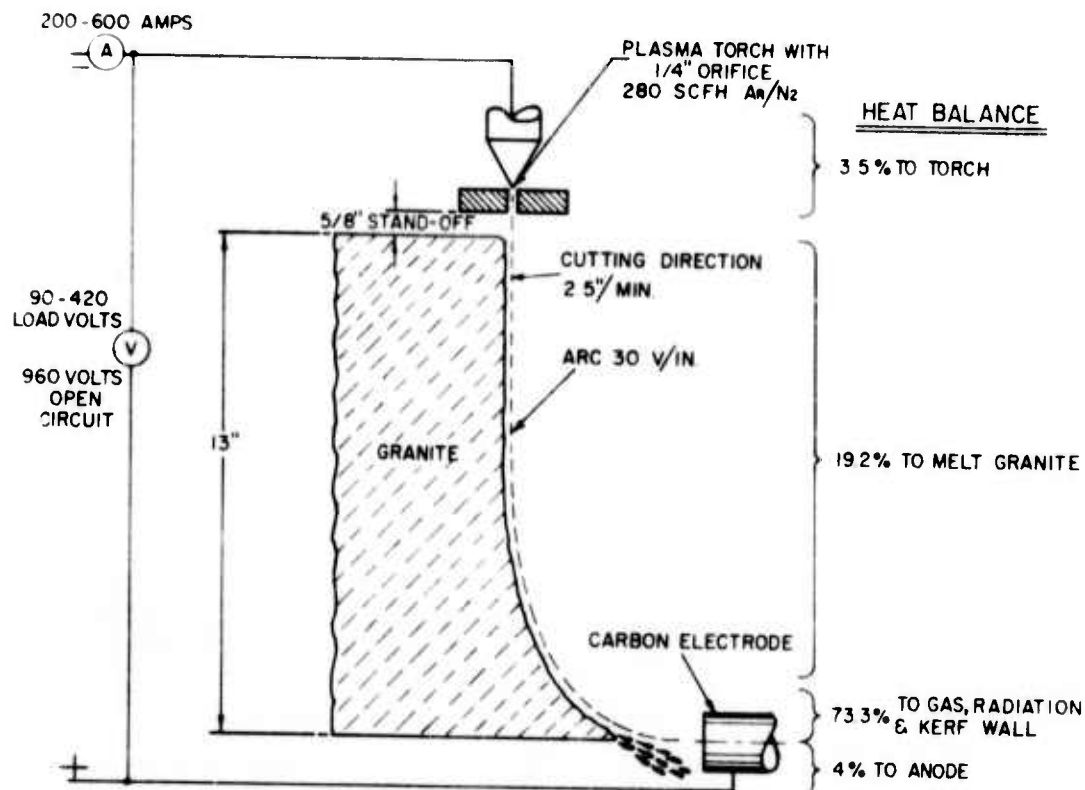
TABLE III (Continued)

Device	Energy Flux Limiting Law	Conditions and Assumptions	Measured or Calculated Heat Flux to Surface (Flux-watts/m ²)
Arc Image Furnace	$E = eK_r T^4$	ADL-Strong Source $r = 0.45$ cm	0.014×10^8
CW Laser		$E = 400$ watts $r = 0.4$ cm Gaussian	0.1×10^8
Pulsed Laser		$E = 5$ joules $t = 10^{-4}$ sec $r = 0.03$ cm	70×10^8



THERMAL TUNNELING
WITH PLASMA TORCHES

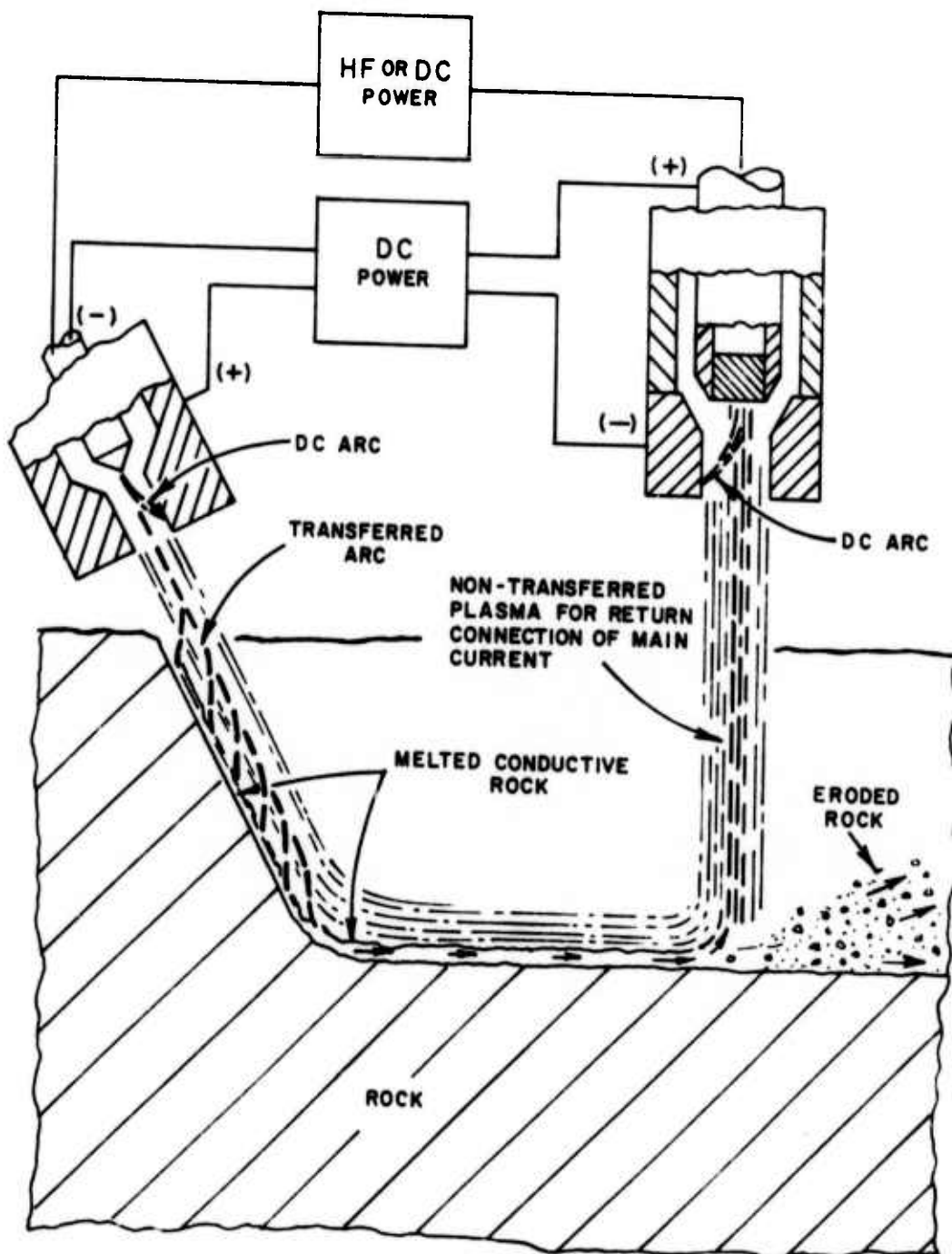
FIG. 1



TYPICAL END VIEW OF KERF

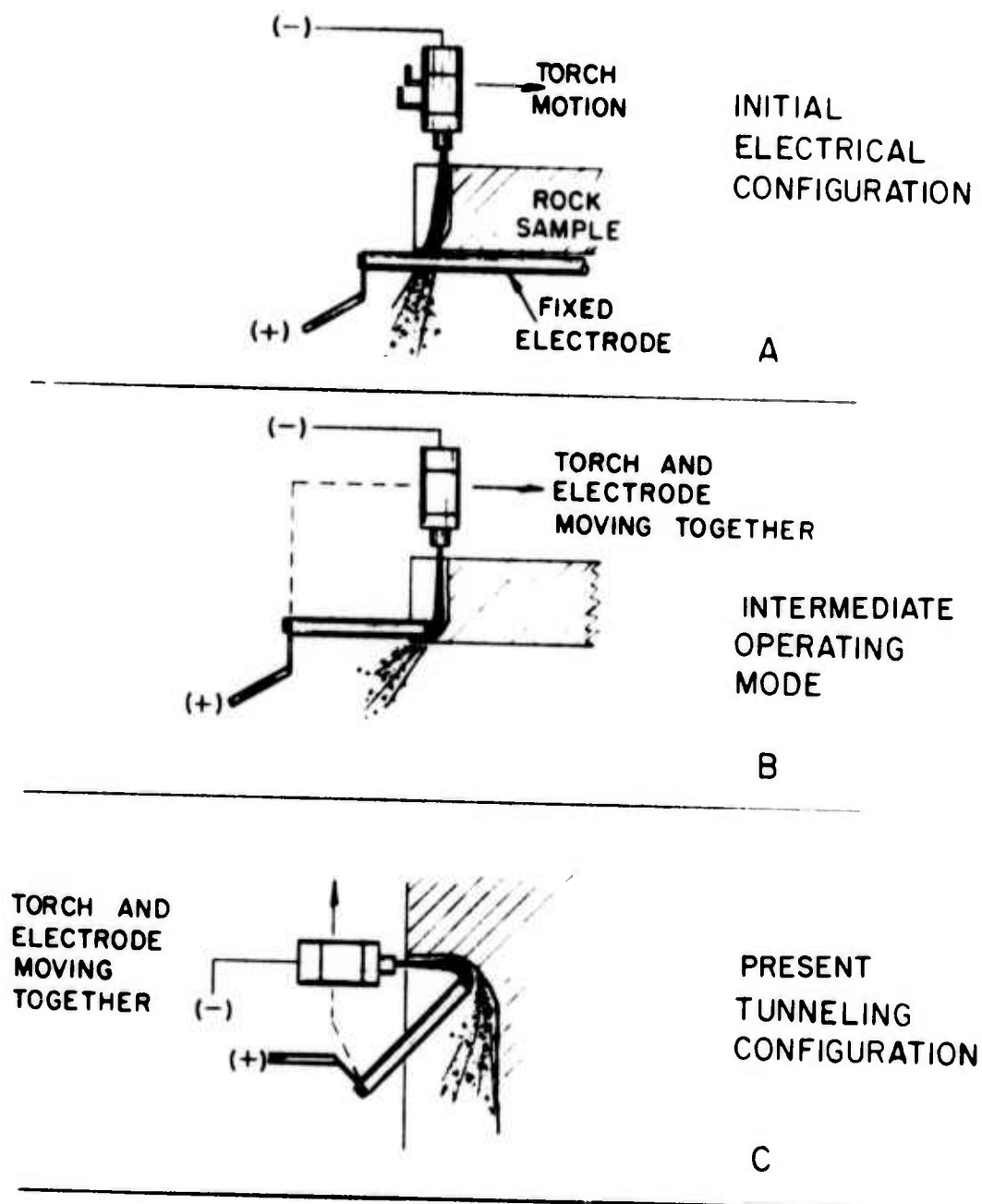
SCHEMATIC AND PERFORMANCE OF PRESENT ARC PLASMA SAW

FIG. 2



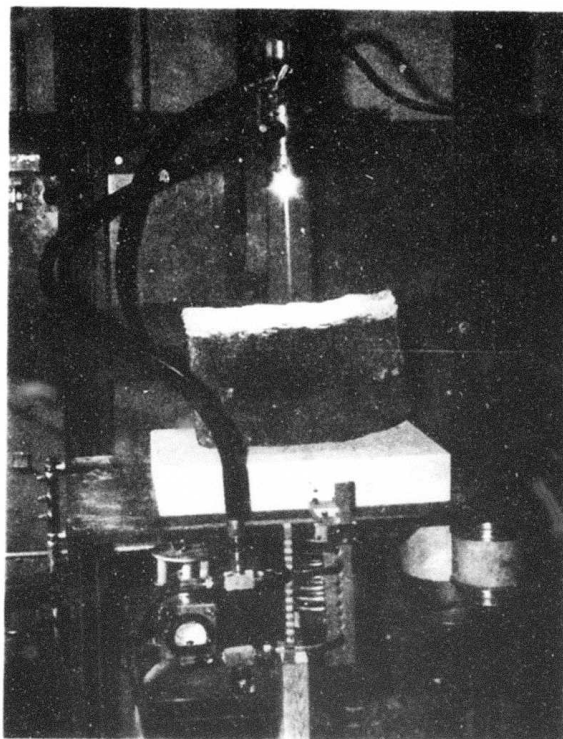
TRANSFERRED ARC CUTTING OF HARD ROCK

FIG. 3

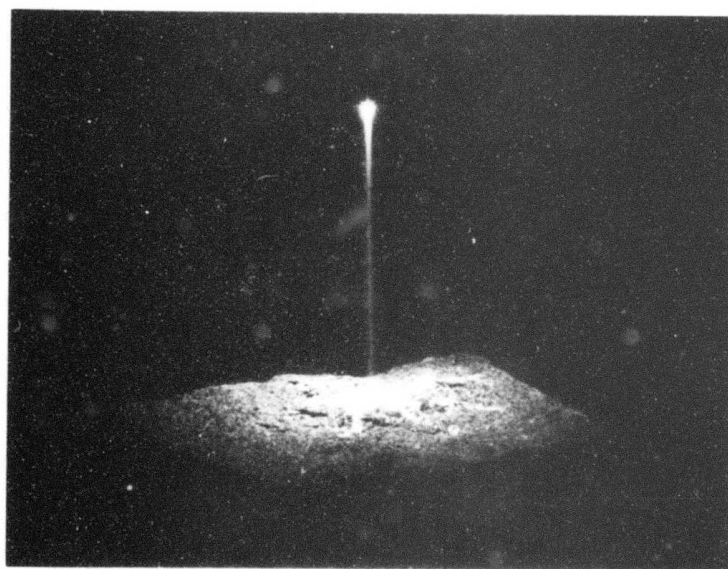


TRANSFERRED ARC OPERATING CONFIGURATIONS

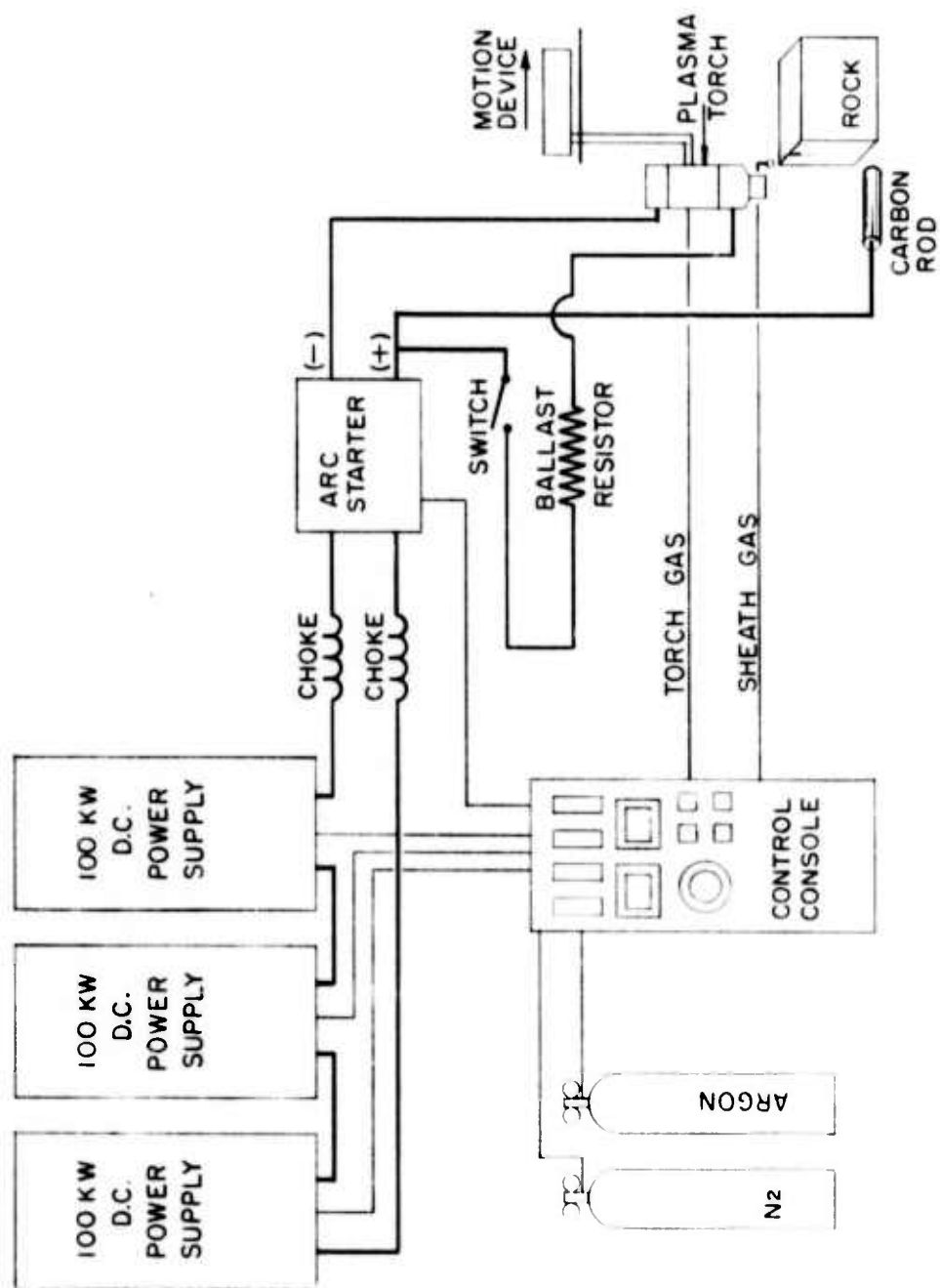
FIG. 4



DIELECTRIC ROCK FRACTURING SETUP SHOWING PLASMA CONTACT
FIG. 5A

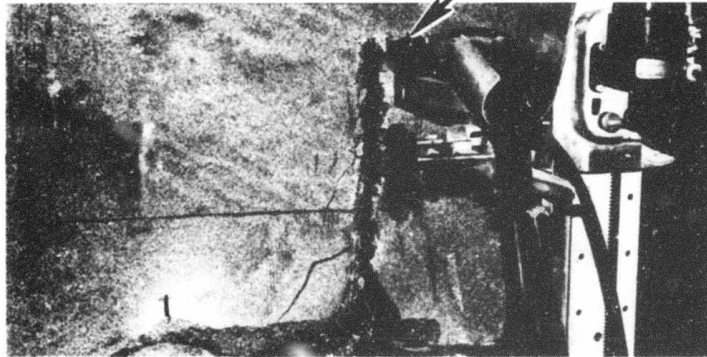


CLOSEUP OF PLASMA CONTACT AND ROCK SURFACE
SHOWING SURFACE ARC TRACKS
FIG. 5B

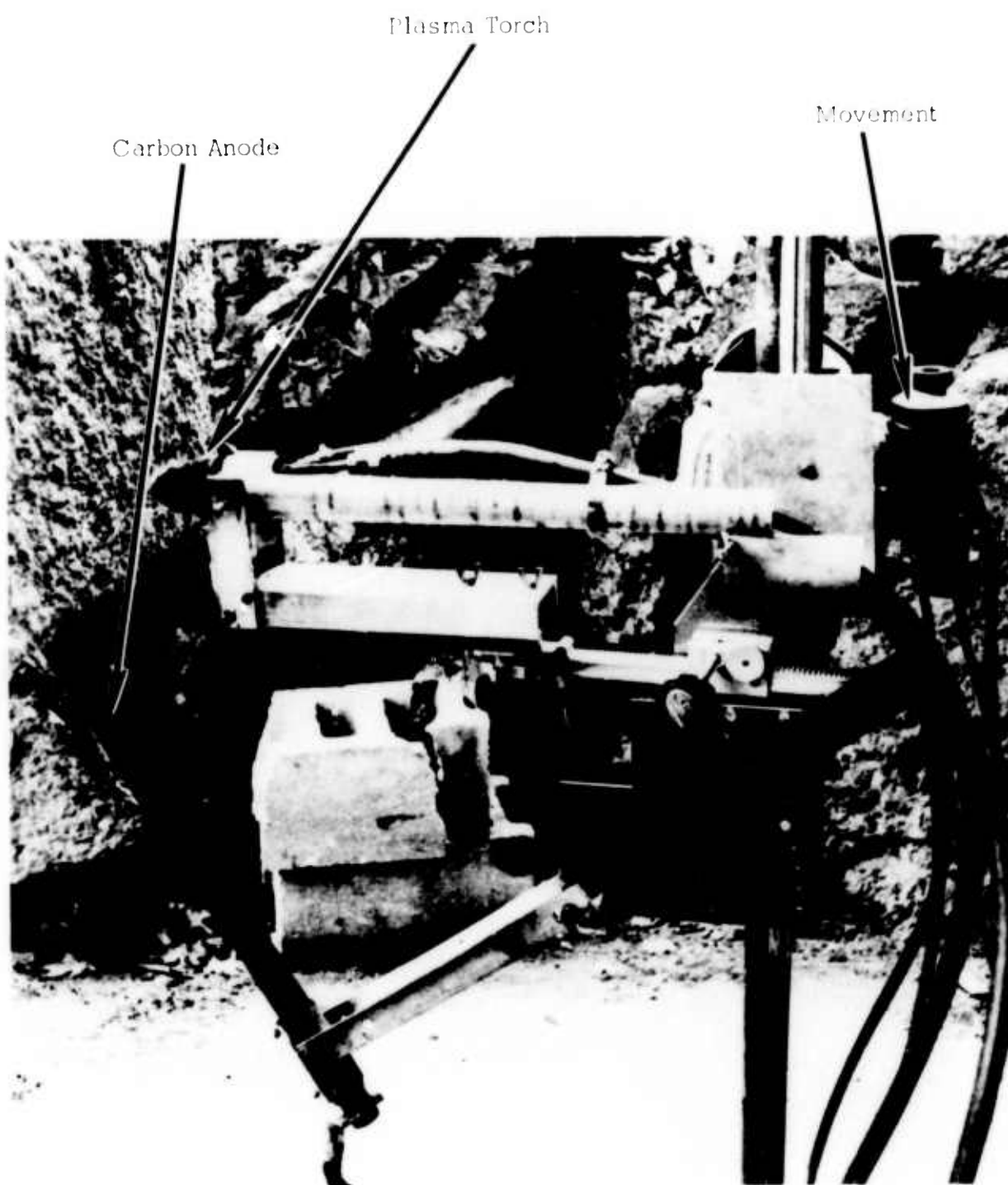


SCHEMATIC OF TRANSFERRED ARC SETUP
FIG. 6

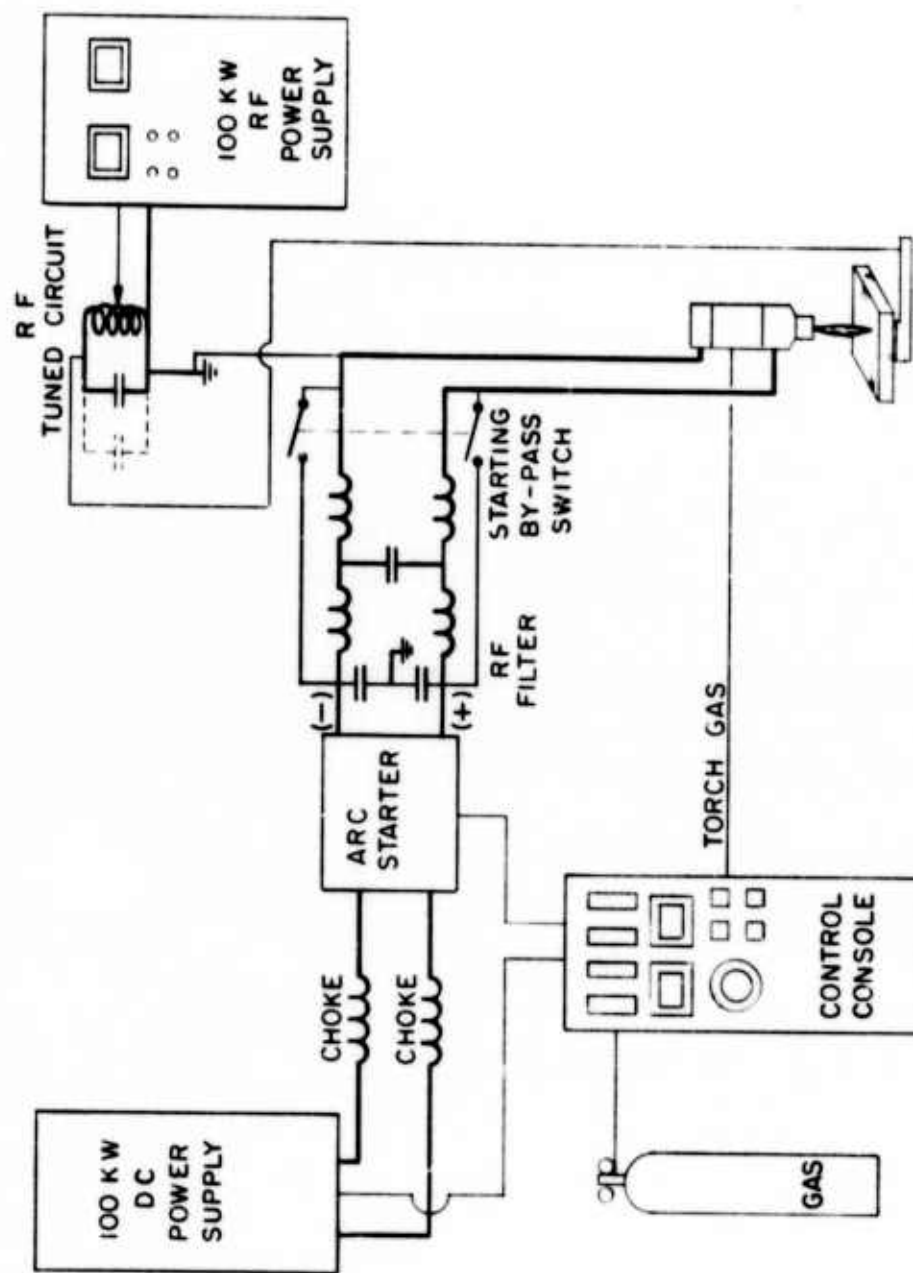
Plasma Torch



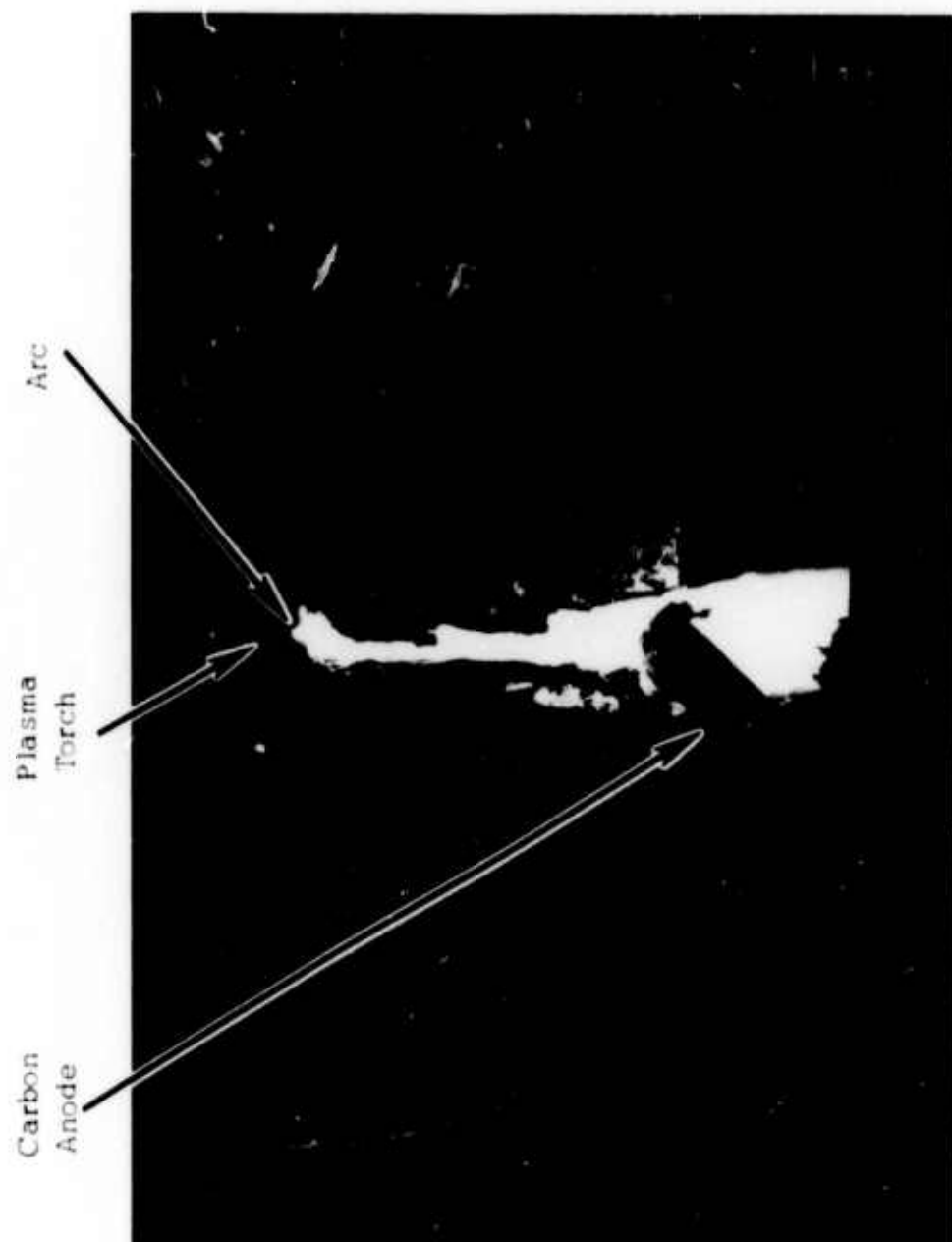
VIEW OF ROCK CUTTING AREA
FIG. 7



TUNNELING CONFIGURATION - ARC PLASMA SAW
FIG. 8



SCHEMATIC OF DIELECTRIC HEATING SETUP
FIG. 9

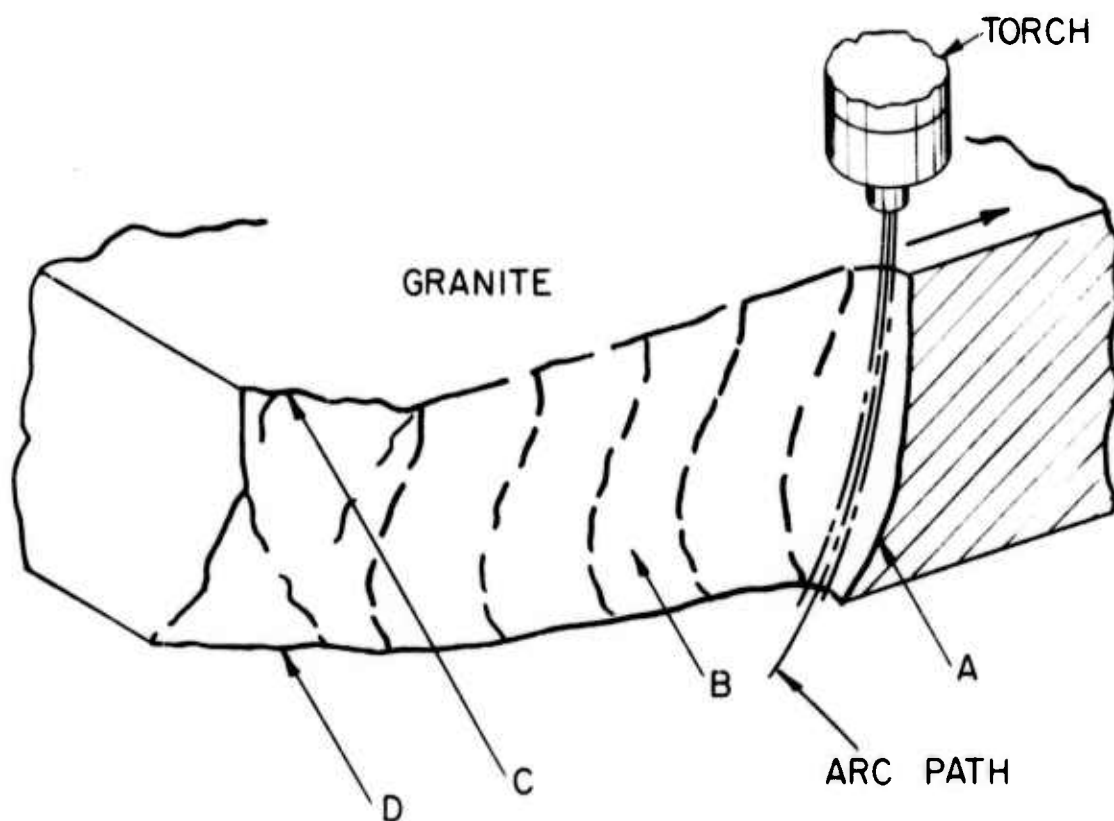


TYPICAL CUTTING OPERATION IN GRANITE

FIG. 10

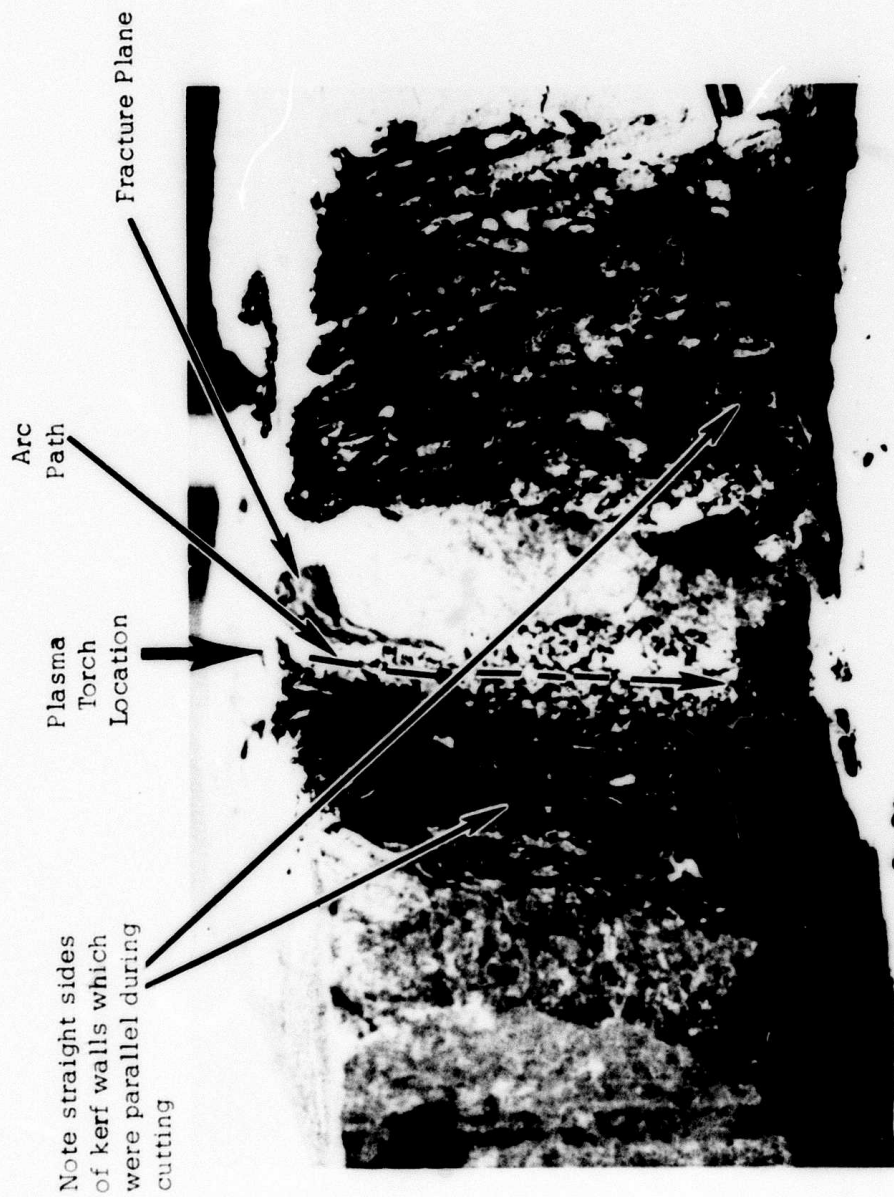


PHOTOGRAPH OF TYPICAL CUT IN GRANITE
FIG. 11

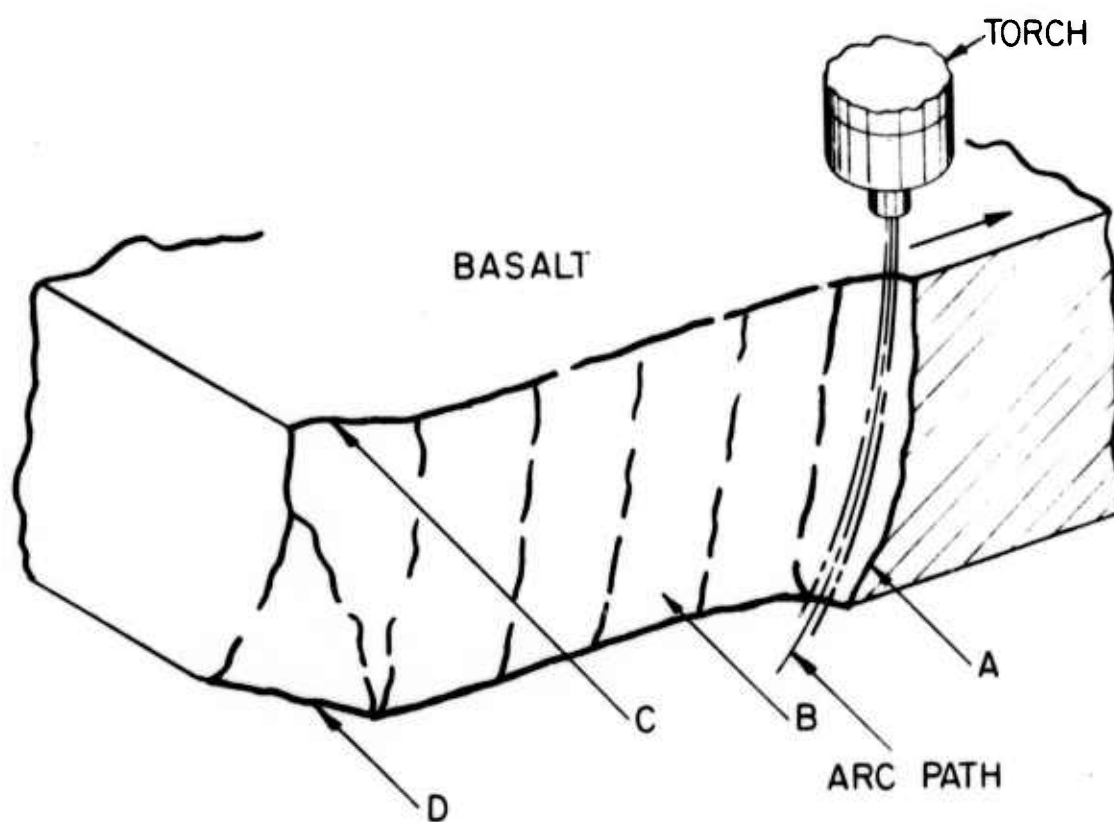


RENDITION OF A CUT IN GRANITE

FIG. 12

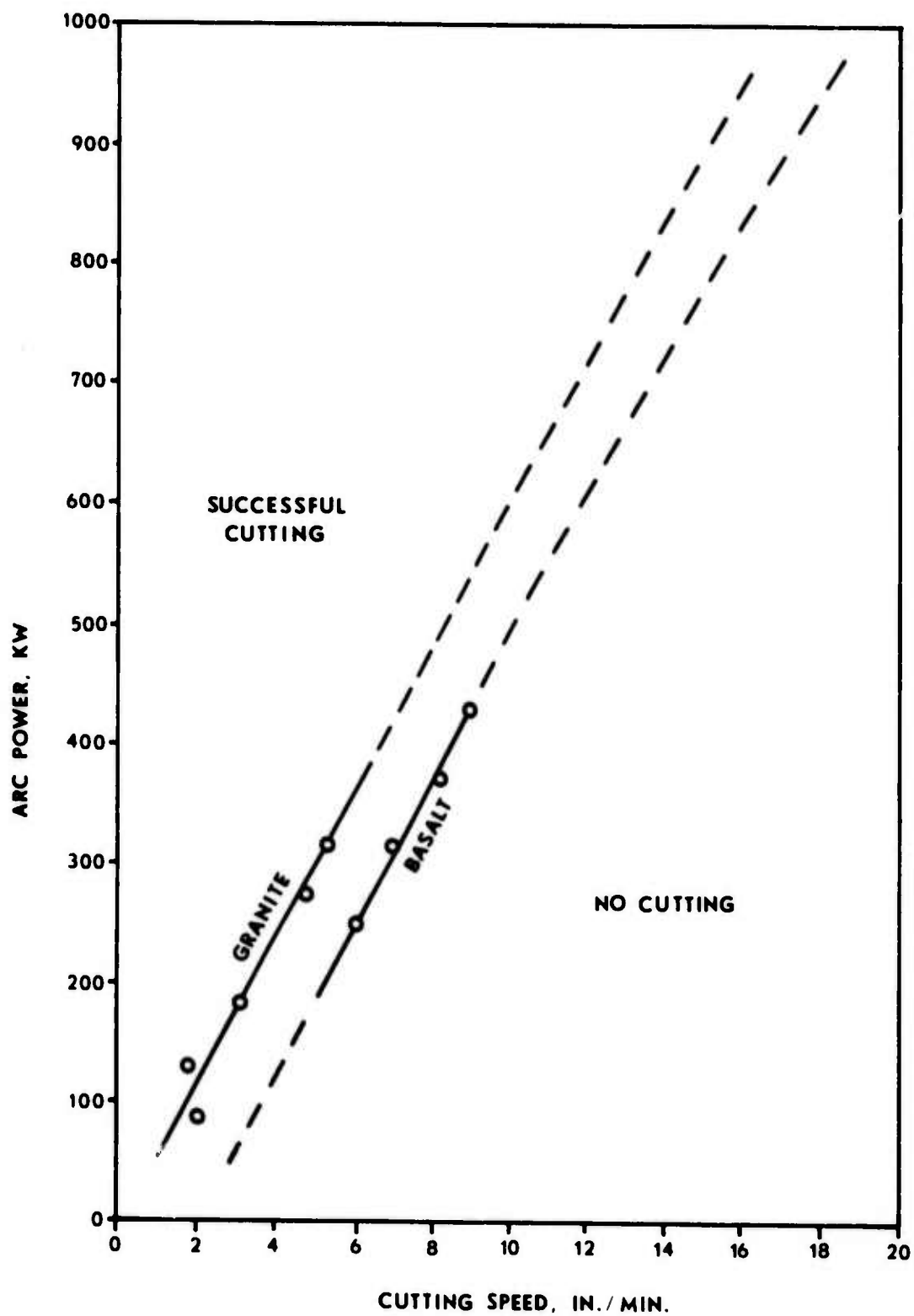


CUT IN DRESSER BASALT (ROCK SPLIT OPEN)

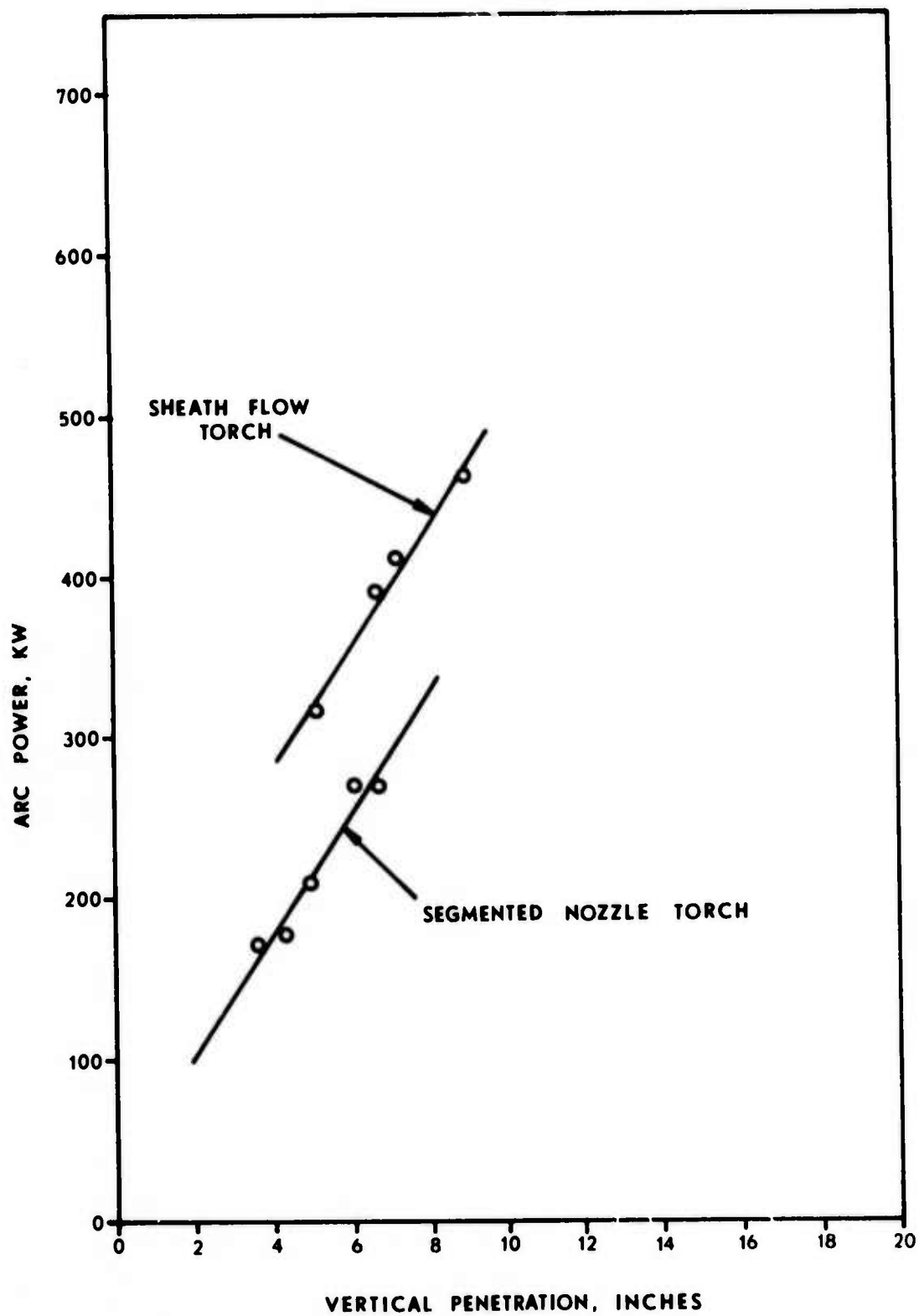


RENDITION OF A CUT IN BASALT

FIG. 14

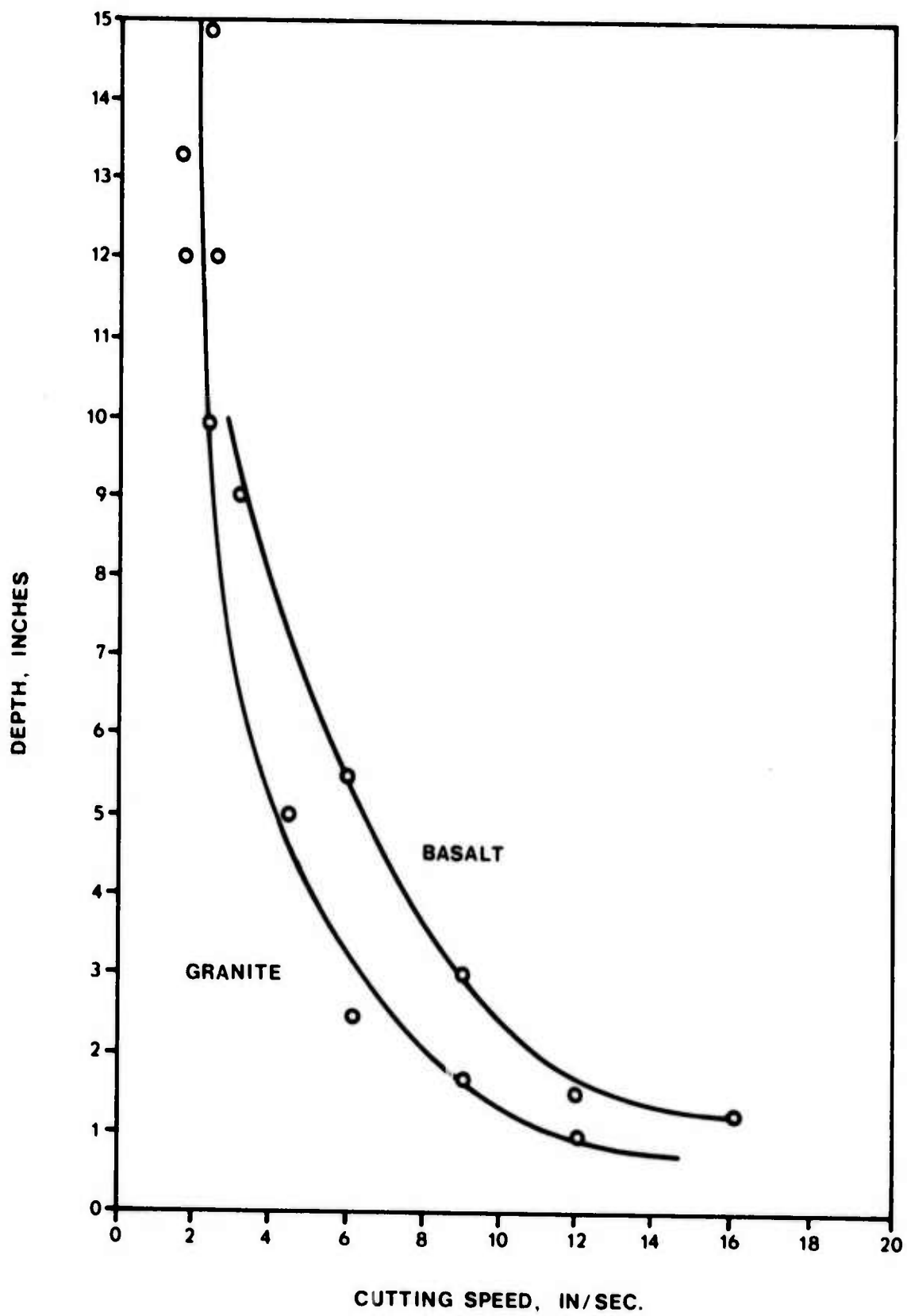


VARIATION OF CUTTING SPEED WITH ARC POWER
USING 3" THICK SAMPLES & NITROGEN PLASMA GAS
FIG. 15



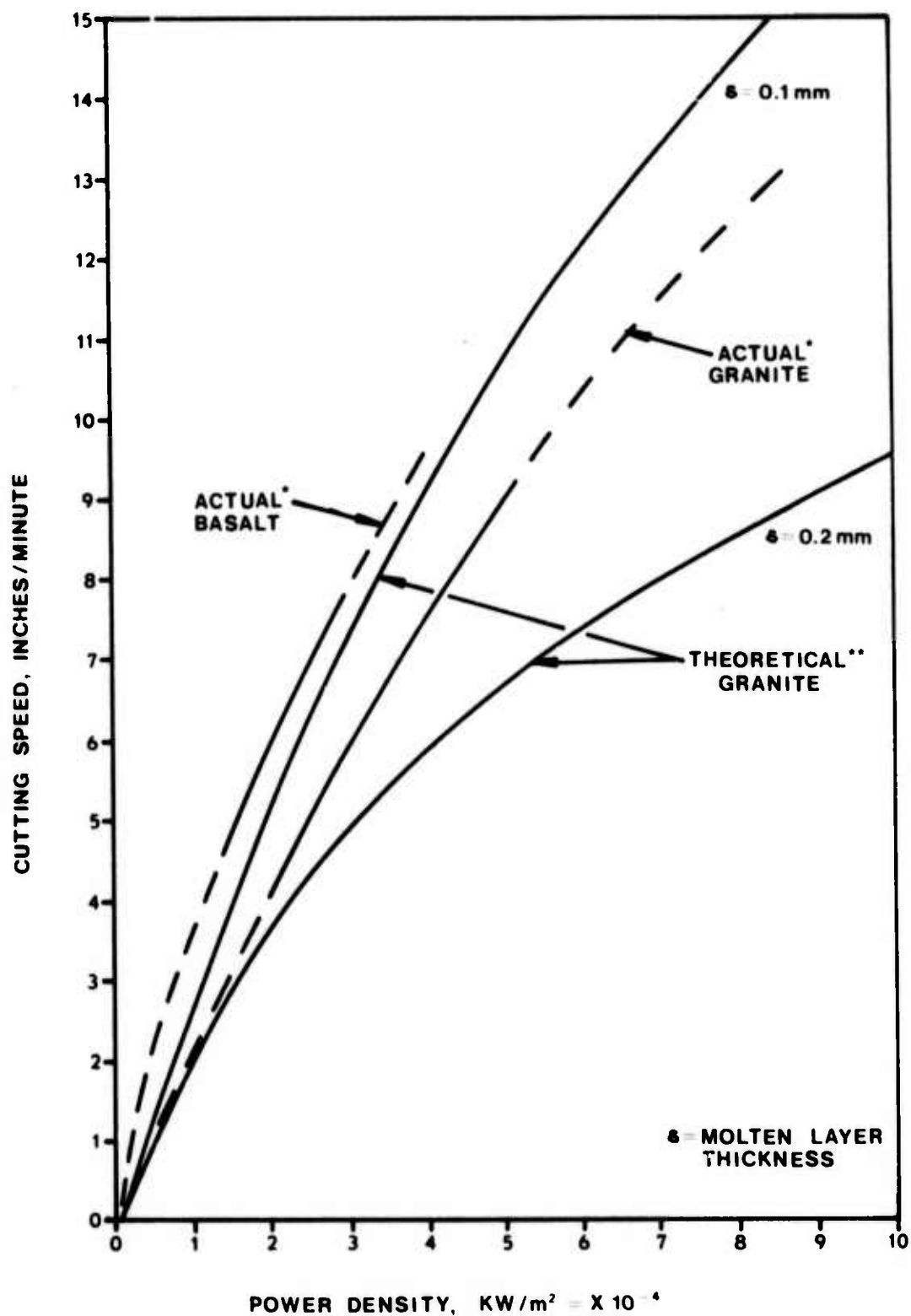
VARIATION OF VERTICAL CUT PENETRATION WITH
ARC POWER FOR TWO TORCH DESIGNS

FIG. 16



VARIATION OF MAXIMUM CUTTING SPEED WITH
CUT DEPTH AT 250 KW

FIG. 17



* ESTIMATED FROM ARC DIMENSIONS MEASURED, ASSUMES 50% ENERGY TRANSFER FROM ARC COLUMN TO ROCK

** THEORETICAL CURVES FOR GRANITE FROM APPENDIX A

VARIATION OF CUTTING SPEED WITH HEAT FLUX TO MELT SURFACE

FIG. 18

68

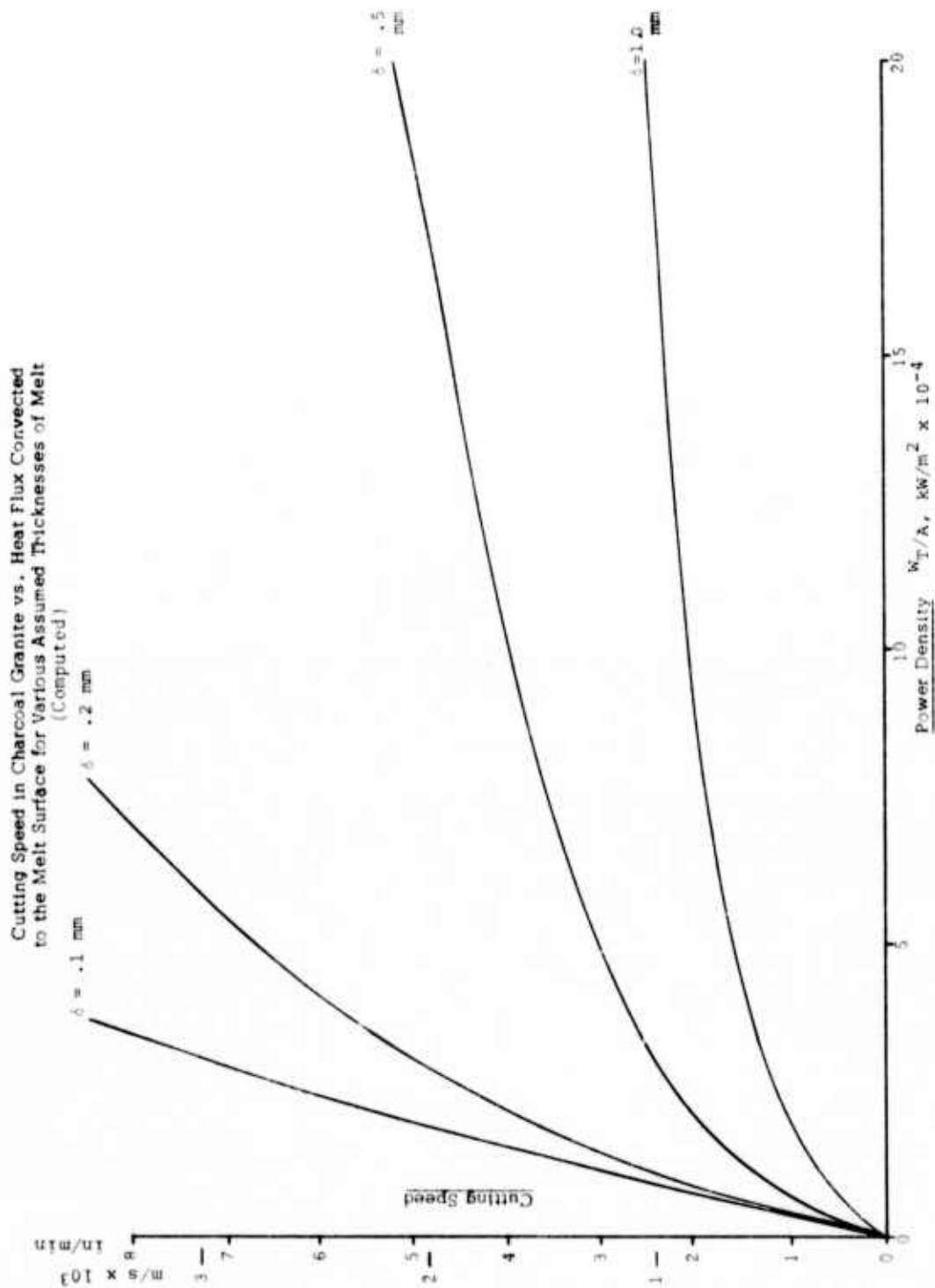
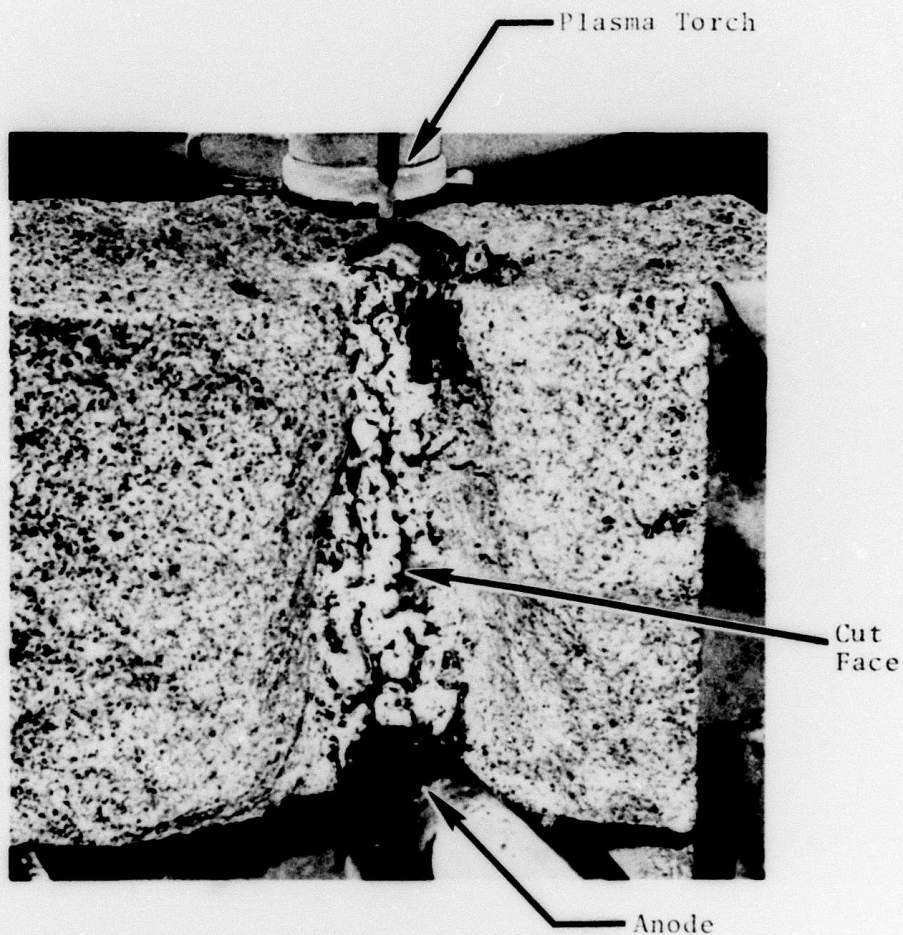
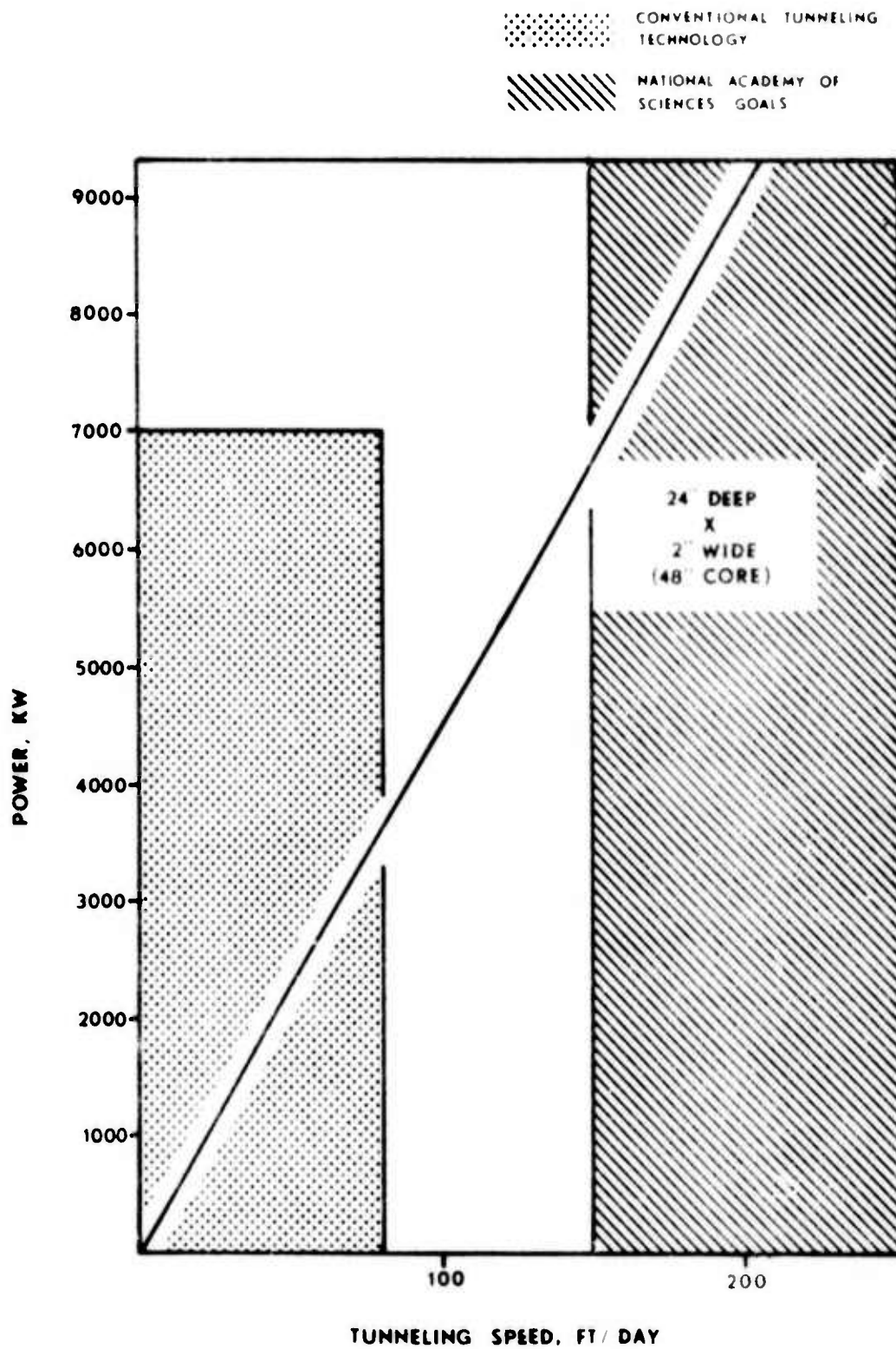


FIG. 19



**PHOTOGRAPH SHOWING WEBB NATURE OF MELT
SURFACE ON CUT FACE**
FIG. 20



PLASMA CUTTER TUNNELING SPEED
FIG. 21



PHOTOGRAPH OF TWO PARALLEL CUTS
SHOWING THERMAL FRACTURING

FIG. 22

Cutting Speed vs. Heat Actually Conducted Into Rock
for Basalt, Charcoal Granite and Sandstone
(Computed)

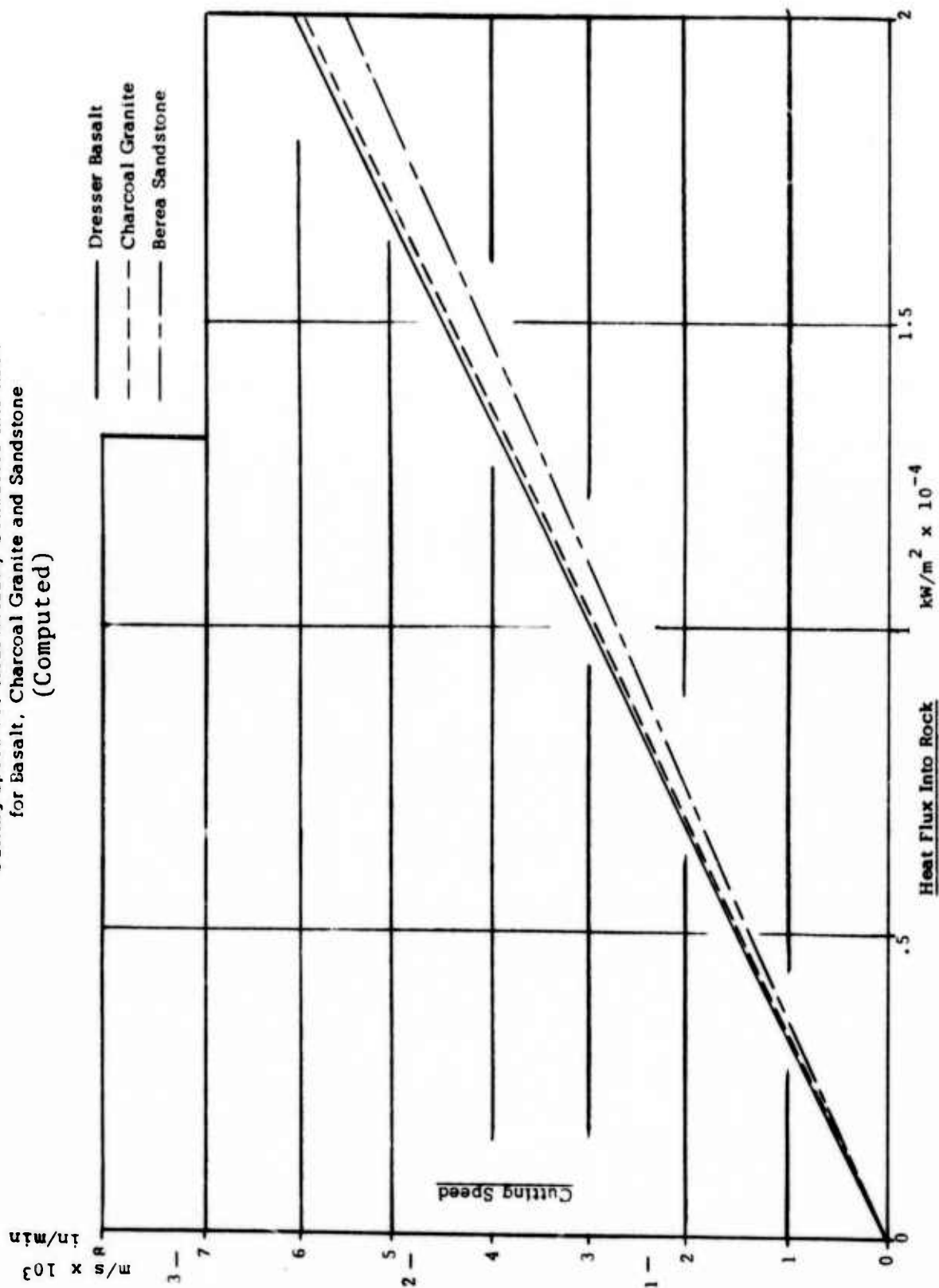


FIG. 23 73

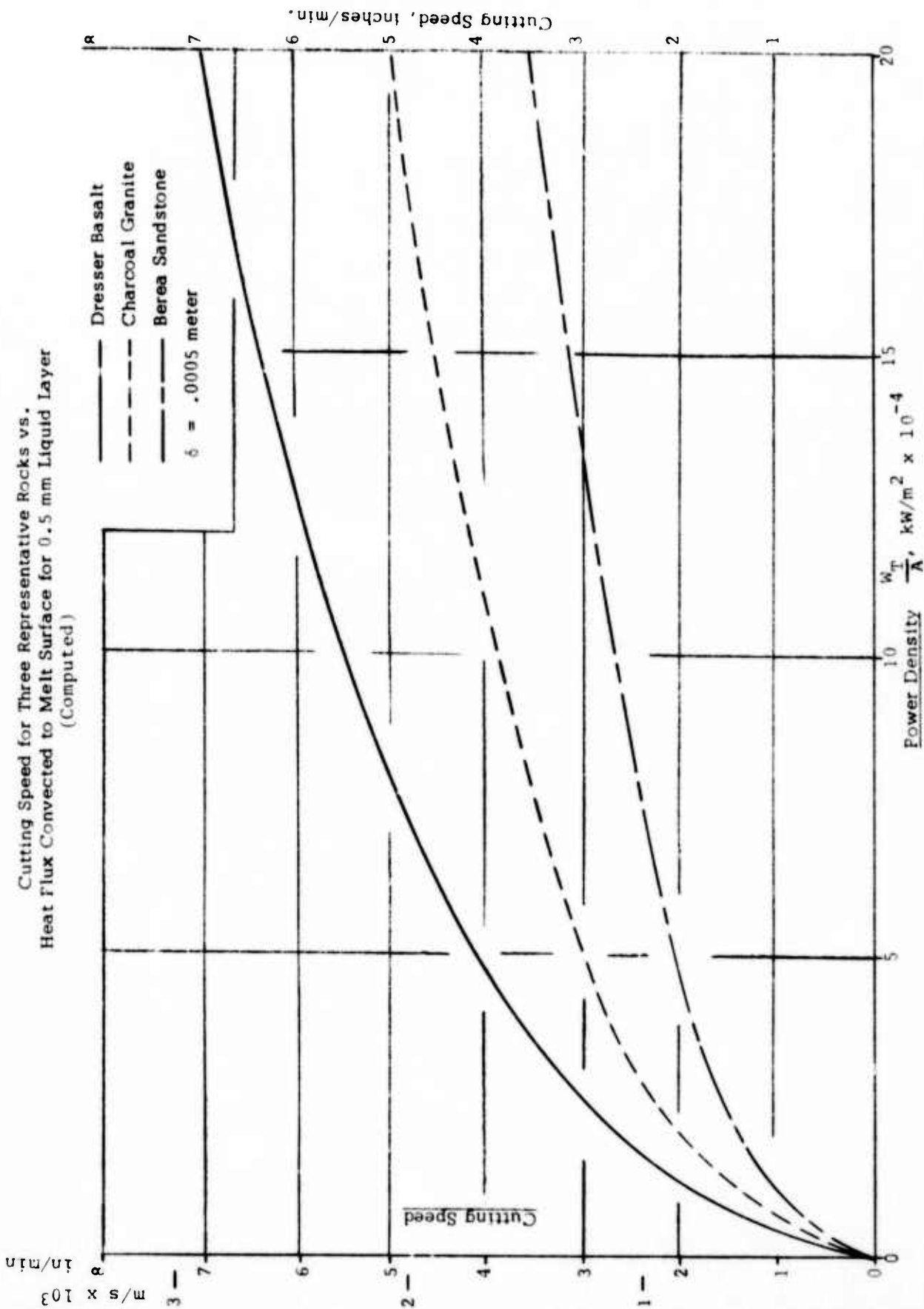


FIG. 24 74

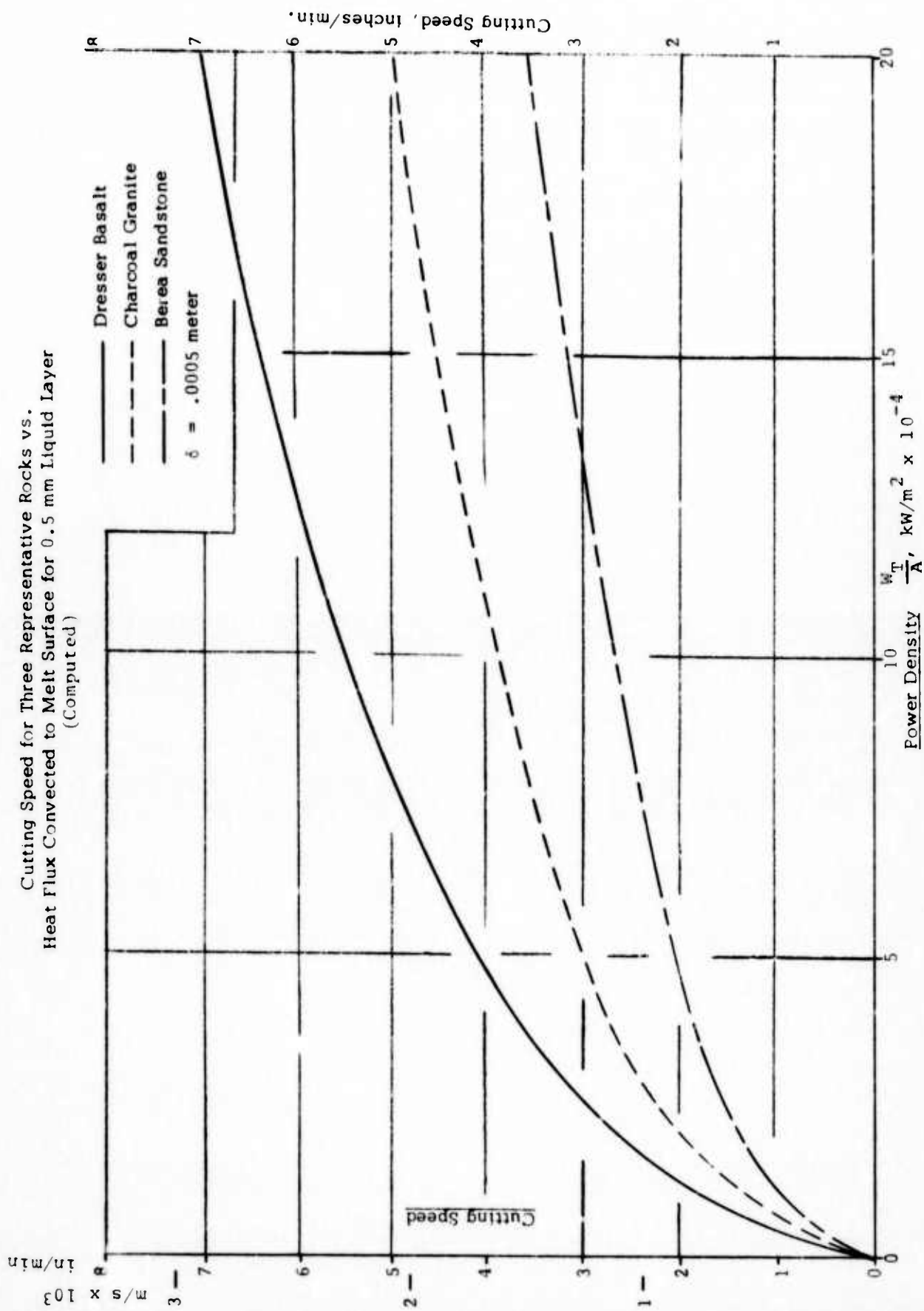
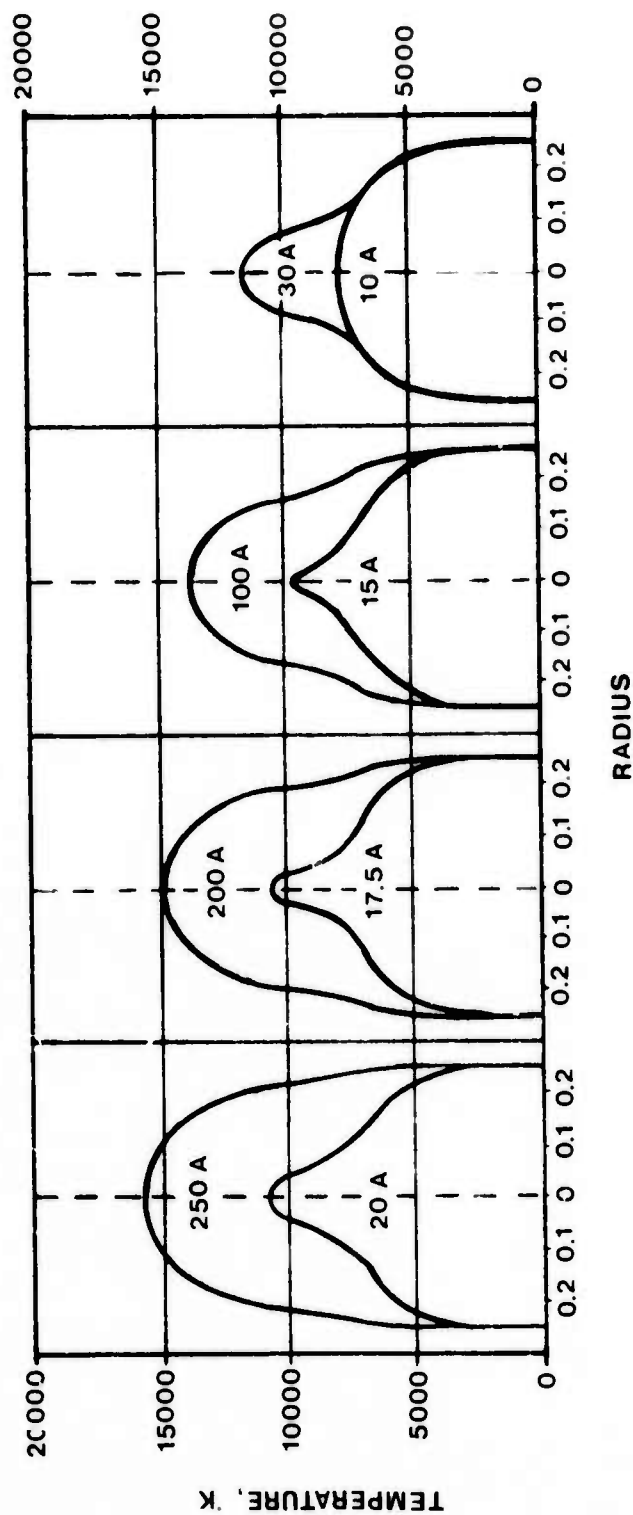
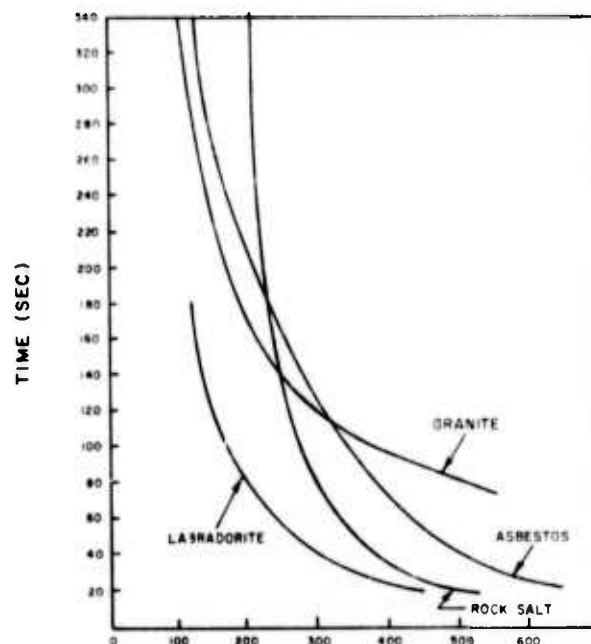


FIG. 24 74

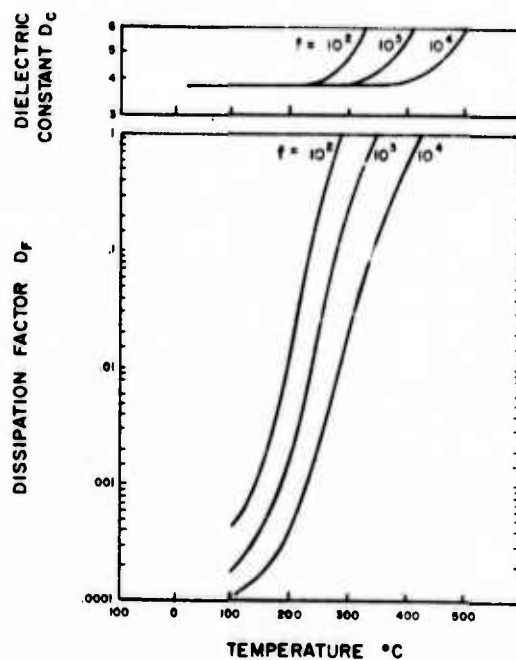


TEMPERATURE VS. RADIUS FOR A 5 mm DIAMETER WATER
COOLED NITROGEN ARC AT VARIOUS CURRENT LEVELS
FIG. 25



TIME REQUIRED FOR CRUSHING ROCK VIA THERMAL INCLUSION
AS FUNCTION OF THE ELECTRIC FIELD STRENGTH (3-6 MHz)

FIG. 26



DIELECTRIC CONSTANTS OF FUSED QUARTZ (24)
(f = FREQUENCY H_z)

FIG. 27